



# Holed up, but thriving: Impact of multitrophic cryoconite communities on glacier elemental cycles

Runa Antony<sup>a,b,\*</sup>, Dattatray Mongad<sup>c</sup>, Aritri Sanyal<sup>a</sup>, Dhiraj Dhotre<sup>c</sup>, Meloth Thamban<sup>a</sup>

<sup>a</sup> National Centre for Polar and Ocean Research, Ministry of Earth Sciences, Vasco-da-Gama, India

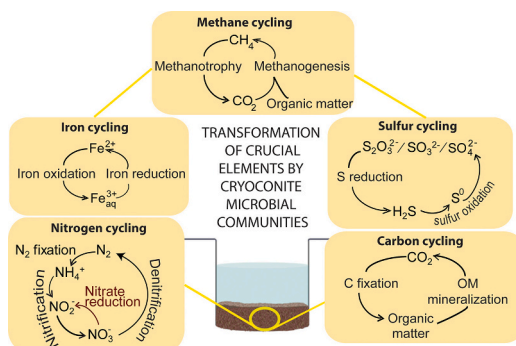
<sup>b</sup> GFZ German Research Centre for Geosciences, Potsdam, Germany

<sup>c</sup> National Centre for Microbial Resource, National Centre for Cell Science, Pune, India

## HIGHLIGHTS

- Functional diversity of cryoconite ecosystems assessed in Antarctica and the Himalayas.
- Methanogenic and methanotrophic communities co-exist and cycle methane.
- Cryoconite microbes have the potential for complete iron cycling through iron oxidation and reduction reactions.
- Region-specific adaptations influence the potential for sulfur, carbon, and nitrogen cycling.

## GRAPHICAL ABSTRACT



## ARTICLE INFO

Editor: Frederic Coulon

### Keywords:

Biogeochemical cycling  
Functional predictions  
Marker-gene studies  
Antarctica  
Himalayas

## ABSTRACT

Cryoconite holes (water and sediment-filled depressions), found on glacier surfaces worldwide, serve as reservoirs of microbes, carbon, trace elements, and nutrients, transferring these components downstream via glacier hydrological networks. Through targeted amplicon sequencing of carbon and nitrogen cycling genes, coupled with functional inference-based methods, we explore the functional diversity of these mini-ecosystems within Antarctica and the Himalayas. These regions showcase distinct environmental gradients and experience varying rates of environmental change influenced by global climatic shifts. Analysis revealed a diverse array of photosynthetic microorganisms, including Stramenopiles, Cyanobacteria, Rhizobiales, Burkholderiales, and photosynthetic purple sulfur Proteobacteria. Functional inference highlighted the high potential for carbohydrate, amino acid, and lipid metabolism in the Himalayan region, where organic carbon concentrations surpassed those in Antarctica by up to 2 orders of magnitude. Nitrogen cycling processes, including fixation, nitrification, and denitrification, are evident, with Antarctic cryoconite exhibiting a pronounced capacity for nitrogen fixation, potentially compensating for the limited nitrate concentrations in this region. Processes associated with the respiration of elemental sulfur and inorganic sulfur compounds such as sulfate, sulfite, thiosulfate, and sulfide suggest the presence of a complete sulfur cycle. The Himalayan region exhibits a higher potential for sulfur cycling, likely due to the abundant sulfate ions and sulfur-bearing minerals in this region. The capability for

\* Corresponding author at: Interface Geochemistry, GFZ German Research Centre for Geosciences, Building A71, Room 224, Telegrafenberg, 14473 Potsdam, Germany.

E-mail address: [rantony@gfz-potsdam.de](mailto:rantony@gfz-potsdam.de) (R. Antony).

<https://doi.org/10.1016/j.scitotenv.2024.173187>

Received 11 December 2023; Received in revised form 10 May 2024; Accepted 10 May 2024

Available online 13 May 2024

0048-9697/© 2024 The Authors. Published by Elsevier B.V. This is an open access article under the CC BY license (<http://creativecommons.org/licenses/by/4.0/>).

complete iron cycling through iron oxidation and reduction reactions was also predicted. Methanogenic archaea that produce methane during organic matter decomposition and methanotrophic bacteria that utilize methane as carbon and energy sources co-exist in the cryoconite, suggesting that these niches support the complete cycling of methane. Additionally, the presence of various microfauna suggests the existence of a complex food web. Collectively, these results indicate that cryoconite holes are self-sustaining ecosystems that drive elemental cycles on glaciers and potentially control carbon, nitrogen, sulfur, and iron exports downstream.

## 1. Introduction

Glaciers serve as critical ecosystems that influence the global climate and hydrology. Within these icy landscapes, cryoconite holes represent unique microhabitats of biogeochemical significance (Fountain et al., 2004; Hodson et al., 2007; Tieber et al., 2009; Sanyal et al., 2018; Segawa et al., 2020; Pittino et al., 2023). Cryoconite holes are water-filled cavities that form when dark granular sediment (cryoconite) that contains biological and mineral components settle on the ice surface, melting the ice beneath them and creating a water-filled hole with the sediment at its base (Cook et al., 2016). Cryoconite holes have a spatially variable but widespread distribution on the ice surface (Fountain et al., 2004; Hodson et al., 2007) and are enriched in organic carbon (Sanyal et al., 2018), nutrients (Bagshaw et al., 2013), and trace metals (Fortner and Lyons, 2018; Singh et al., 2017a). Due to its dark color, cryoconite is efficient at attracting solar energy, impacting the radiative and optical properties of the glacier where it accumulates, and therefore accelerates glacier melting (Takeuchi et al., 2001; Di Mauro et al., 2017). As cryoconite holes and surface melt pools are often connected to the near-surface hydrologic system, their contents can be transported via the drainage system to downstream environments and the glacier bed (Fountain et al., 2004). They also accumulate radioactive isotopes and anthropogenic pollutants with great efficiency, acting as a sink for these pollutants on the glacier until the glacier retreats and cryoconite melting releases them into the surrounding environment (Baccolo et al., 2017). Despite their small size, cryoconite holes play important roles in the carbon, nitrogen, sulfur, and nutrient cycles (Anesio et al., 2009; Telling et al., 2011; Cameron et al., 2012; Segawa et al., 2020; Pittino et al., 2023), weathering of minerals (Sanyal et al., 2020), and melting of the ice (Takeuchi et al., 2001; Oerlemans et al., 2009). Cryoconite microbial communities, through their metabolic activity, can exert a significant influence on the biological and chemical properties of meltwater collected on the glacier surface (Sanyal et al., 2018; Samui et al., 2020) and redistributed through melting.

Glaciers worldwide are undergoing unprecedented changes, such as glacier retreat, ice shelf calving, and large-scale changes to surface hydrology as atmospheric temperatures continue to rise (Siegert et al., 2019; King et al., 2020). Among these, mountain glaciers, particularly the Himalayan glaciers, which constitute one of the world's largest renewable supplies of freshwater that sustain the livelihood of millions of people (Schaner et al., 2012), are particularly vulnerable (Naegeli and Huss, 2017). The dramatic physical, geochemical, and biological changes experienced by glaciers due to a warming climate will likely impact the metabolism and biogeochemical capacities of the microbial communities residing within these icy landscapes. In the backdrop of climate-driven transformations of glacier environments, the influence of cryoconite hole microbes on the chemistry of the water held within the holes and routed through complex near-surface hydrological networks (Fountain et al., 2004; MacDonell et al., 2016) becomes even more pronounced. It is, therefore, important to understand the range and consequences of biogeochemical potentials of resident microbes. Knowledge of microbial processes in these environments would also help us better predict the impacts of climate change on glacier ecosystems. Thus, in this study, the functional potential of cryoconite communities corresponding to major ecological processes of carbon, nitrogen, sulfur, and iron cycling was determined in the contrasting environments of Antarctica and the Himalayas, which are characterized

by different environmental gradients (temperature, altitude, precipitation, and solar radiation) and experience different rates and magnitudes of environmental change. This was done by targeted analysis of functional marker genes encoding key enzymes that catalyze the biogeochemical reactions of carbon and nitrogen cycling, together with functional predictions of cryoconite communities from high throughput 16S rRNA data. Our study of microbial communities and biogeochemical processes across these geographically distinct regions offers new insights into their roles in ecosystem processes and their contribution to the biotic and chemical properties of the glacier surface environment. Moreover, through this comparative study, we elucidate microbes and ecological processes that are universal across different glacier systems while also uncovering region-specific adaptations.

## 2. Methods

### 2.1. Field site and sample collection

Cryoconite hole sediment samples were collected from 15 open cryoconite holes along an altitudinal transect ranging from 4630 to 5051 m above mean sea level in the Sutri Dhaka glacier in the Lahaul-Spiti region of the western Himalayas. The areal extent of the glacier is approximately 25 km<sup>2</sup> and trends from southwest to northeast (Fig. 1). The climate in this region is characterized by a transition zone of monsoonal to arid climate regime (Bookhagen and Burbank, 2010). Two distinct zones were delineated within the Himalayan transect: HIM1 (lower ablation zone), below 4900 m and marked by heavy debris cover and high melt rates, and HIM2 (upper ablation zone), situated above 4900 m, distinguished by low debris cover and lower melting rates. A total of 11 open cryoconite holes were sampled from the HIM1 region and 4 open holes from the HIM2 region. Fewer samples were collected from the HIM2 region, situated at higher elevations, due to logistical

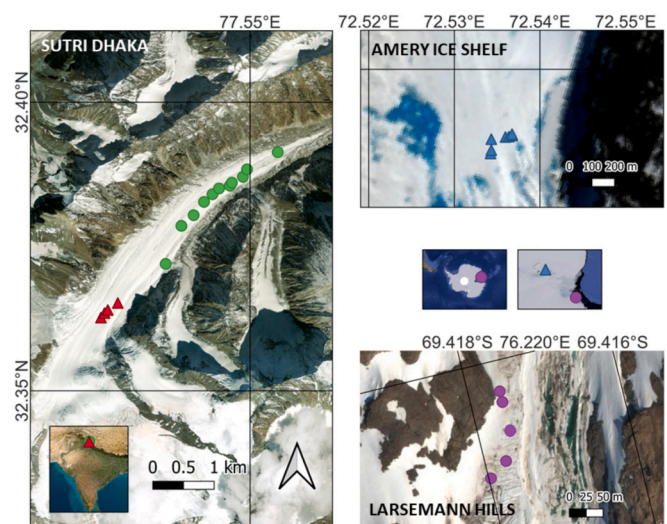


**Fig. 1.** Location of samples collected from Larsemann Hills (purple circles) and Amery Ice Shelf (blue triangles) in East Antarctica and the Sutri Dhaka glacier in Western Himalayas. Samples collected above 4900 m amsl in the Sutri Dhaka glacier are shown in red triangles, while those from altitudes below 4900 m are in green circles.

challenges that constrained our sampling efforts in this area. Between 10 and 100 g of debris (wet weight) was collected from each cryoconite hole. Samples were collected into sterile acid-cleaned HDPE bottles, stored frozen in the field, and transported to the laboratory on dry ice.

Samples were also collected from 5 randomly selected cryoconite holes in the Grovnes peninsula, Larsemann Hills (LHS), and 7 in the Amery Ice Shelf (AIS), East Antarctica, from locations shown in Fig. 1. Sampling at these locations was carried out at near sea level. Despite sampling several cryoconite holes from the LHS, only 5 provided adequate cryoconite sediment for all analyses conducted in this study. In AIS, limited helicopter time and access difficulties restricted our ability to collect additional samples. Debris collected from each cryoconite hole weighed <2 g (wet weight). The sampling site at LHS is located within a coastal valley that receives a significant influx of debris from adjacent bedrock surfaces. The cryoconite holes in this region experience a dynamic interchange of nutrients, organic carbon, and microbes due to their hydrological connection with supraglacial meltwater (Samui et al., 2018). Cryoconite holes here predominantly remain open, primarily fed by snowmelt and water channels during summer. In contrast, cryoconite holes within the AIS are characterized by sealed ice lids and are frozen solid. These holes are isolated from each other and exhibit an enrichment in inorganic solutes and organic carbon (Samui et al., 2018). Located over 100 km from the coast, these cryoconite holes lie within a blue ice area near the Jennings Promontory, marking the eastern boundary of the AIS. Marine sea spray inputs heavily influence surface ice environments in both LHS and AIS (Antony et al., 2011; Samui et al., 2017). Sediment in cryoconite holes from LHS was collected in sterile WhirlPak bags. Cryoconite holes in the AIS were frozen and were sampled using a KOVACS Mark IV coring device. Samples were immediately transported on ice to the research base and stored at  $-20^{\circ}\text{C}$  until analysis. In the laboratory, frozen cryoconite hole core samples were melted at  $4^{\circ}\text{C}$  in sterile WhirlPak bags. Melted water was siphoned off, leaving the sediment at the base.

## 2.2. Geochemical measurements

For analysis of inorganic ions, wet sediment was suspended in 5 ml MilliQ water, sonicated for 5 min, and spun down at  $3000 \times g$  for 30 min. The supernatant was diluted 4 times in MilliQ water and analyzed for cations and anions on a Thermo Fisher ICS 5000+ HPIC ion chromatography system. For the analysis of total organic carbon, homogenized cryoconite hole sediment was oven-dried overnight at  $60^{\circ}\text{C}$ , finely ground, and acidified with 2 N hydrochloric acid before analysis using a Shimadzu TOC-V SSM-5000A organic carbon analyzer.

## 2.3. DNA extraction, amplification, and sequencing of functional marker genes

Sediment samples from each site, within respective locations (i.e., LHS, AIS, HIM1, and HIM2), were pooled together so that each sample was equally represented in the homogenized mixture used for community genomic DNA extraction. DNA was extracted from 0.8 g replicate subsamples from the pooled, homogenized sediments using a MoBio Soil Extraction Kit following the manufacturer's instructions. Replicate DNA samples were pooled for library preparation, yielding a final concentration of 4.6  $\mu\text{g}$ , 1.5  $\mu\text{g}$ , 4.0  $\mu\text{g}$ , and 3.3  $\mu\text{g}$  of DNA from LHS, AIS, HIM1, and HIM2, respectively, as quantified using a nano spectrophotometer (Eppendorf).

Functional marker genes for carbon fixation (cbbLR, rbcL), nitrogen fixation (nifH), nitrification (bacteria- and archaea-specific AmoA), and various steps of the denitrification pathway, i.e., nitrate reduction (narG), nitrite reduction (nirS), nitric oxide reduction (qnorB) and nitrous oxide reduction (nosZ) were amplified using polymerase chain reaction (PCR) conditions detailed in the supplementary file and primers and listed in Table S1. The PCR products containing the correct fragment size were purified using Wizard SV Gel and PCR Clean-Up kit (Promega).

DNA fragments amplified by PCR were ligated directly into the pCR4-TOPO vector following the manufacturer's protocols. Single colonies growing on a selective solid medium were screened for the correct insert size using PCR primers T3 and T7 (see supplementary methods for details). The plasmid containing the desired insert was purified using PureLink Quick Plasmid Miniprep Kit (Invitrogen) and sequenced using a gene analyzer AB3730  $\times$  1. The sequences were assembled and edited using Sequencher V4.10.1 (GeneCodes) and screened for chimeras using the DECIPHER tool (<http://decipher.cee.wisc.edu/FindChimeras.html>). Taxonomic assignments were performed using the NCBI database.

## 2.4. GenBank accession numbers

Gene sequences obtained in this study have been deposited in the GenBank database under the accession numbers: OL422343 to OL422348 (CbbLR), OL422354 to OL422416 (rbcL), OL422184 - OL422342 (bacteria-specific AmoA), OL422182-OL422183 (archaea-specific AmoA), OL422349- OL422350 (narG), and OL422351-OL422353 (nosZ).

## 2.5. Illumina MiSeq sequencing

The 16S rRNA gene universal bacterial primers 515F/806R (Caporaso et al., 2012) that targets the V4 hypervariable region was used to analyze cryoconite bacterial diversity. Amplification of the V6 hypervariable region of archaeal 16S rRNA genes was carried out using V6-major (958arcF/1048arcR-major) and V6-minor (958arcF/1048arcR-minor) primer sets (Cameron et al., 2015). Amplification of the eukaryotic 18S rRNA V9 hypervariable region was achieved using the F1380/F1389/R1510 primer set (Cameron et al., 2015). The fungal-specific primer pairs ITS1F/ITS2 (Smith and Peay, 2014) and ITS3/ITS4 (White et al., 1990), which target the ITS1 and ITS2 regions, respectively, were used for the characterization of the fungal communities. A two-step PCR approach was used to generate amplicon libraries for Illumina sequencing (Kozich et al., 2013). The amplicon libraries were purified with Agencourt AMPure beads (Beckman Coulter Genomics) and the library concentration for Illumina MiSeq was quantified using the Quant-iT PicoGreen dsDNA Assay (Invitrogen).

## 2.6. Illumina data analysis

Quality control checks were performed on raw sequence data with FastQC (v0.11.5). Sequences were filtered to eliminate primers and adapter sequences from sequencing reads using Cutadapt (v1.18) before merging the forward and reverse reads. The overlapping paired-end Illumina reads were assembled into full-length sequences using PEAR (v0.9.10). Also, all sequence reads that were too short (<100 bp long) or had ambiguous base calls were removed. Chimeric sequences were discarded using VSEARCH (v2.4.2) based Greengenes (v13.5) and UNITE (v7.2) databases for 16S rRNA and ITS sequences, respectively. For the whole data set, we obtained 1,146,361 assembled sequences (on average, 57,318 sequences per sample) post-quality control. Bacterial and archaeal sequences were assigned to operational taxonomic units (OTUs) using a closed reference-based OTU picking method in QIIME (v1.7) using the Greengenes database. For eukaryotic sequences (V9 region), closed reference-based OTU picking with SILVA (v132) was performed. For ITS sequence reads, OTUs were picked using the open reference method with the UNITE (v7.2) database. The sequences are available in the NCBI Short Read Archive (SRA) under the BioProject accession number PRJNA825340.

Alpha diversity indices and beta diversity analysis were carried out in R (version 3.4.2, R Core Team, 2017, Vienna, Austria) using phylosEq (v1.20.0), vegan (v2.3.5), and ggplot2 (v2.1.0). The abundance data underwent Hellinger transformation using the microbiome package in R (v.4.3.2). Subsequently, a non-metric multidimensional scaling (NMDS) plot was generated using Euclidean distance on the transformed data to



depict the differences between samples graphically. The similarity percentages (SIMPER) analysis was run using the PAST3 tool (Hammer-Muntz et al., 2001) to identify which OTUs contribute most to differences between the Himalayan and Antarctic microbial communities. Based on classified sequences, we determined the functional potential associated with the identified bacterial communities using the Functional Annotation of Prokaryotic Taxa (FAPROTAX, Louca et al., 2016) and phylogenetic investigation of communities by reconstruction of unobserved states (PICRUSt, Langille et al., 2013) KEGG database. The relative abundances of inferred pathways were tested for normality using a Shapiro-Wilk test. If the  $p$ -value was  $<0.05$ , the null hypothesis of normality was rejected, indicating that the populations were not normally distributed. Subsequently, a Kruskal-Wallis test was conducted to examine variations in the abundance of inferred pathways among the sites, followed by Dunn's test for multiple comparisons using rank sums alone. Correction of  $p$ -values was done using the Benjamini-Hochberg method. The BugBase algorithm (Ward et al., 2017) was used to predict bacterial phenotypes, and the resulting dataset was evaluated for significant differences in bacterial phenotypes between groups using the Mann-Whitney-Wilcoxon test, which is a standard approach within the BugBase platform.

### 3. Results

#### 3.1. Geochemical conditions across the glaciers

The chemistry of the cryoconite hole sediments in LHS, Antarctica, was  $\text{Ca}^{2+}\text{-Na}^+\text{-Cl}^-$  ion dominated with contributions from  $\text{K}^+$ ,  $\text{Mg}^{2+}$ , and  $\text{SO}_4^{2-}$ . The Himalayan cryoconite sediments were  $\text{Ca}^{2+}\text{-Na}^+\text{-K}^+$  dominated.  $\text{Mg}^{2+}$ ,  $\text{NO}_3^-$ ,  $\text{Cl}^-$ ,  $\text{NH}_4^+$ , and  $\text{SO}_4^{2-}$  also contributed to the major ion chemistry of the Himalayan cryoconite (Table 1). High total organic carbon concentrations characterized the cryoconite hole sediments from the Himalayan region with values 1 to 2 orders higher than that in LHS. In general, cryoconite from the upper ablation region was characterized by higher inorganic ion and organic carbon concentrations than from the lower ablation region. Sediment chemistry was not determined for the AIS due to sample limitations.

#### 3.2. Taxonomic composition of the microbial communities

##### 3.2.1. Bacteria

Analysis of the taxonomic composition of bacteria in cryoconite sediment from both Antarctic locations showed that Cyanobacteria dominated, accounting for 33–50 % of the OTUs (Fig. 2A). Among the Cyanobacteria, Pseudanabaenales was present at a high relative abundance in both LHS and AIS, with Oscillatoriales being additionally observed in LHS. Other dominant phyla in both Antarctic samples were Proteobacteria (17–25 %), Bacteroidetes (11–16 %), and Actinobacteria (10 %). Acidobacteria were prevalent in the AIS (11 %) and were less commonly observed in LHS (0.7 %). Other phyla that co-occurred in both samples at low abundances are shown in Fig. 2A and Table S3.

The predominant communities in the Himalayan cryoconite were Cyanobacteria (9.6–43.2 %), Proteobacteria (22.6–40.1 %), and Bacteroidetes (14.1–37.1 %). Cyanobacteria in the Himalayan cryoconite comprised Pseudanabaenales, Oscillatoriales, and Synechococcales,

with abundances  $5\times$  higher in the lower ablation than in the upper ablation zone (Table S3). Among the other sequences that co-occurred in both Himalayan habitats, Armatimonadetes, Firmicutes, Acidobacteria, and Chloroflexi were in high abundance. At the same time, Proteobacteria and Bacteroidetes were present at lower abundances in the lower ablation zone.

##### 3.2.2. Eukarya

Based on the eukaryotic SSU rRNA gene analysis, Metazoa (Animalia) and the fungi Ascomycota were the dominant taxa in the Antarctic LHS and AIS sample (Fig. 2B, Table S4). Metazoa and Ascomycota accounted for 96 % and 86 % of the OTUs in LHS and AIS, respectively.

Other Eukaryotic taxa that were present in both the Antarctic samples were Cercozoa (Amoeboids and Flagellates), Ciliophora (Ciliates), Discicristata (Amoeboflagellates), Ochrophyta (Algae) and Chlorophyta (Algae). The Himalayan lower ablation zone cryoconite communities were dominated by fungi, with Ascomycota and Basidiomycota together accounting for 98 % of OTUs. In contrast, these fungal communities had lower abundances of  $<11$  % in the upper ablation zone. By analyzing the fungal ITS region (ITS1 and ITS2), we were able to detect the presence of other fungi, such as Chytridiomycota and Monoblepharomycota (Fig. 2C, D and Tables S5, S6). Other eukaryotic taxa, such as Peronosporomycetes (water molds, 22.2 %) and cercozoa (17.5 %), were predominant in the upper ablation area and were rarely observed in the lower ablation region. Eukaryotic taxa commonly observed in both the Himalayan samples but at low abundances ( $< 5$  %) were Cercozoa, Ciliophora, Metazoa, and Chlorophyta.

##### 3.2.3. Archaea

Archaea were detected only in cryoconite from the upper ablation region of the Himalayas and comprised members of the phyla Euryarchaeota and Crenarchaeota. Euryarchaeota predominantly consisted of sequences related to Methanoregulaceae (96.7 %), Halobacteriaceae (2.6 %), and Methanomassiliococcaceae (0.1 %). The phyla Crenarchaeota comprising Nitrososphaeraceae constituted about 0.2 % of the archaeal sequences (Table S7).

#### 3.3. Variation of microbial community composition

A comparison of microbial composition showed that 7 % of the OTUs were common to all four habitats. These include eukaryotic sequences related to Cercozoa, Chlorophyta, Metazoa (Animalia), Ascomycota, and Basidiomycota; and bacteria from the phyla Cyanobacteria, Bacteroidetes, Proteobacteria, Actinobacteria, Acidobacteria, Armatimonadetes, Gemmatimonadetes, and Planctomycetes. The genera common between all four sampling sites are listed in Table S8. About 39 % of the OTUs found in the lower ablation zone (HIM1) were also found in the upper ablation zone (HIM2), while 23 % of the OTUs were shared between LHS and AIS. Several OTUs were present at one site only, with more OTUs being uniquely observed in the Antarctic than in Himalayan samples. LHS had the greatest number of unique OTUs (48 % of its total diversity), followed by AIS (41 %), HIM2 (33 %), and HIM1 (27 %). Details of the OTUs unique to each location are provided in Table S9. A non-metric multidimensional scaling plot using Euclidean distance between OTU compositions revealed a clear distinction between the

**Table 1**  
The concentration of major cation, anions, and total organic carbon (TOC) in cryoconite.

Location	Average concentration in $\mu\text{g g}^{-1}$ ( $\pm$ SD)								
	$\text{Cl}^-$	$\text{NO}_3^-$	$\text{SO}_4^{2-}$	$\text{Na}^+$	$\text{NH}_4^+$	$\text{K}^+$	$\text{Mg}^{2+}$	$\text{Ca}^{2+}$	TOC
HIM1 ( $n = 11$ )	46 $\pm$ 30	33 $\pm$ 22	14 $\pm$ 6	150 $\pm$ 101	19 $\pm$ 13	145 $\pm$ 30	59 $\pm$ 9	121 $\pm$ 33	9852 $\pm$ 3587
HIM2 ( $n = 4$ )	62 $\pm$ 14	43 $\pm$ 13	25 $\pm$ 6	201 $\pm$ 102	78 $\pm$ 22	151 $\pm$ 28	68 $\pm$ 13	206 $\pm$ 54	11,114 $\pm$ 2643
LHS ( $n = 5$ )	133 $\pm$ 64	3 $\pm$ 4	14 $\pm$ 8	106 $\pm$ 43	7 $\pm$ 4	58 $\pm$ 21	96 $\pm$ 31	194 $\pm$ 179	941 $\pm$ 583

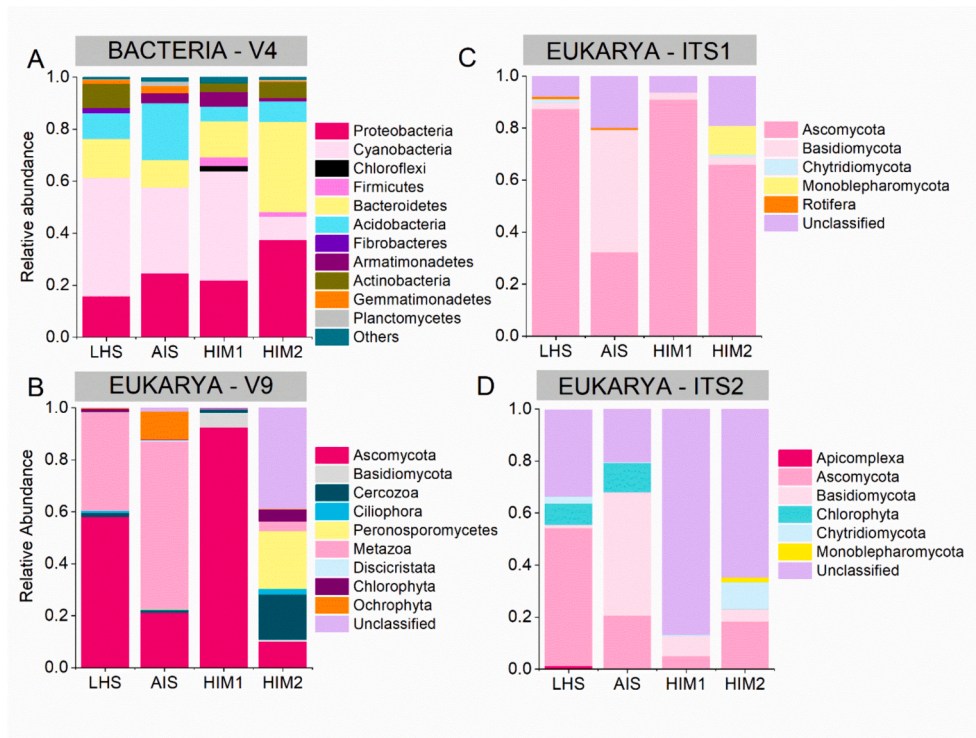


**Fig. 2.** Relative abundance of bacteria at the phylum level (A) and eukaryotes identified by targeting the 18S rRNA V9 hypervariable region (B), ITS1 region (C), and ITS2 region (D) across various samples collected from Antarctica and the Himalayas.

Antarctic and Himalayan samples (Fig. S1). These patterns were further corroborated by SIMPER analysis, which revealed high dissimilarity between the bacterial (overall average dissimilarity 82.72 %), fungal (ITS1-97.84 %, ITS2-98.09 %), and other eukaryotic (95.25 %) microbial communities in the Antarctic and Himalayan glaciers. The bacterial and eukaryotic OTUs that contribute most to the differences between the Antarctic and Himalayan glaciers are shown in Table S10.

### 3.4. Carbon and nitrogen cycling functional genes within cryoconite communities

The large subunit gene (*rbcl*) coding for the enzyme ribulose-1,5-diphosphate carboxylase/oxygenase (RuBisCO) that catalyzes the first step of the CO<sub>2</sub> fixation reaction, where CO<sub>2</sub> is reduced to form organic carbon, was amplified from all the samples. Taxa containing the *rbcl* gene responsible for carbon fixation in the Antarctic samples comprised photosynthetic yellow-green Ochrophyta algae within the Stramenopiles (88.07–99.45 % identity), the cyanobacteria Synechococcales (85.77–87.95 % identity), and photosynthetic purple sulfur proteobacteria of the order Chromatiales (85.34–84.15 % identity). Thirty-five to 60 % of the *rbcl* genes sequenced from the Himalayan cryoconite were related to Stramenopiles (86.63–99.64 % identity) and the rest to Cyanobacteria (83.94–89.97 % identity).

We also determined the diversity of autotrophic bacteria by amplifying the red-like phylogenetic groups of the *cbbL* genes (*cbbLR*) encoding the large subunit of form I RubisCO. The *cbbLR* gene was amplified from the Antarctic sites and the upper ablation zone in the Himalayan region. The *cbbL* gene amplified from AIS was related to Rhizobiales (71.01 %) and Burkholderiales (87.72 %), while sequences from the Himalayan sample showed 87.54 to 87.74 % identity to the *cbbLR* gene from Burkholderiales.

To investigate the presence of a nitrogen-fixing community within cryoconite, we targeted the *nifH* gene, which encodes the enzyme nitrogenase that catalyzes the fixation of atmospheric nitrogen to ammonia. *NifH* genes were amplified from all the cryoconite samples

but showed no significant similarity to sequences in the NCBI database. The presence of a nitrifier community within the cryoconite was determined by targeting the bacterial and archaeal *AmoA* genes that catalyze the oxidation of ammonia. The bacteria-specific *AmoA* gene was amplified from all samples and was related to the *AmoA* gene from *Nitrosospora* (95.09–100.00 % identity) and *AmoA* gene from bacteria with no classification descriptions (90.84–99.80 % identity). The archaea-specific *AmoA* gene was only detected in the AIS sample and did not show similarity to any *AmoA* gene sequences in the database.

The cryoconite communities were also analyzed for the presence of *narG* gene-encoding enzymes that catalyze nitrate reduction to nitrite. The *narG* gene was amplified from the Himalayan lower ablation zone and was most closely related to the *narG* gene from an unidentified bacterial clone at 90.07 to 90.35 % identity. The *nirS* gene associated with the reduction of nitrite to nitric oxide and the nitric oxide reductase gene (*qnorB*) that catalyzes the reduction of nitric oxide to nitrous oxide was not amplified from any sample. Genes associated with the reduction of nitrous oxide to nitrogen gas (*nosZ*) were not detected in the Antarctic samples but were amplified and sequenced from both the Himalayan samples. The *nosZ* gene showed 84.88 to 85.63 % identity to members of the family Bradyrhizobiaceae.

### 3.5. Predicted functional annotation of microbial taxa

High-throughput sequencing of bacterial 16S rRNA genes followed by functional predictions using FAPROTAX and PICRUSt showed that cryoconite supports a metabolically diverse microbial community. We want to stress here that although phylogeny and function are believed to be sufficiently linked to enable insights into functions based on predictions from 16S data and a reference genome database (Langille et al., 2013), these predictive tools potentially underestimated gene frequencies that are of biogeochemical significance (Toole et al., 2021). While these tools cannot replace shotgun metagenomic sequencing, when combined with targeted functional marker gene analysis and supporting information on specific functions from lab-based studies

(enzyme screening, carbon bioavailability experiments, organic substrate utilization assays, etc.) using cultured relatives from the same sites, they can provide valuable first assessments of the functional potential within microbial communities. A considerable number of studies have used this method to estimate bacterial functions in glacier environments (Kim et al., 2017; Toubes-Rodrigo et al., 2021; Ren et al., 2022; Rolli et al., 2022; Zhang et al., 2023) and can be used as a stepping stone for further targeted exploration. Using the PICRUSt 16S marker gene predictions, 47 to 48 % of the predicted genes were attributed to metabolism. The most abundant functional categories in all samples were carbohydrate metabolism ( $7.9 \pm 0.3$  %), amino acid metabolism ( $6.8 \pm 0.2$  %), metabolism of cofactors and vitamins ( $6.3 \pm 0.6$  %), nucleotide metabolism ( $3.2 \pm 0.0$  %) and lipid metabolism ( $2.0 \pm 0.2$  %) (Fig. 3). Kruskal-Wallis test did not show any significant difference in the PICRUSt predicted metabolic functions among the Antarctic and Himalayan glaciers ( $H = 0.16$ ,  $p$ -value 0.98,  $df = 3$ ) or between samples within the same glacier (Himalayas:  $H = 0.06$ ,  $p$ -value 0.80,  $df = 1$ ; Antarctica:  $H = 0.05$ ,  $p$ -value 0.81,  $df = 1$ ).

In addition, functional predictions were performed using FAPROTAX, which provides information on the biogeochemical functions of bacteria. Functional categories present in all the 4 sites were those related to phototrophy (13.6–23.8 %), chemoheterotrophy (2.7–20.0 %), photoheterotrophy (0.9–8.7 %), fermentation (1.1–11.5 %), methylophony (0.06–0.20 %), chitinolysis (0.002–0.4 %), cellulolysis (0.03–0.3), and hydrocarbon degradation (0.01–0.1) (Fig. 4). The relative abundance of these major pathways was consistent across all sites (Kruskal-Wallis test:  $H = 1.10$ ,  $df = 3$ ,  $p$ -value = 0.7). However, the less common pathways showed a significant difference in their relative abundances ( $H = 8.32$ ,  $df = 3$ ,  $p$ -value = 0.04; Fig. 4). Subsequent Dunn testing for the low abundance pathways indicated significant variability only between sites HIM1 and HIM2 ( $z = 22.89$ ,  $p$ -value = 0.04). The potential for heterotrophy and carbon degradation was higher in the Himalayan upper ablation site than in the others, while that for phototrophy and photoautotrophy was lower in the upper ablation region. These differences were however not statistically significant ( $H = 3$ ,  $df = 3$ ,  $p$ -value = 0.39; Fig. 4).

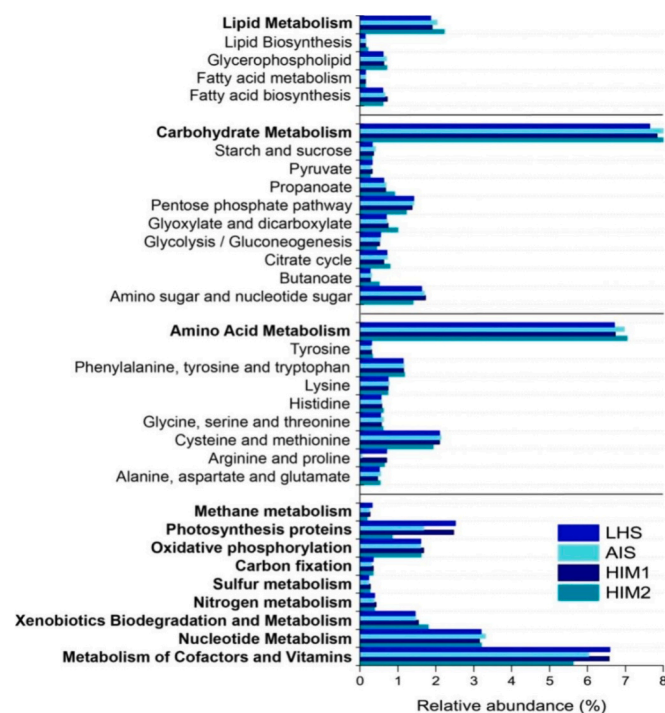


Fig. 3. PICRUSt predictions of the functional composition of cryoconite microbiome.

Sulfur cycling potentials were particularly high in the Himalayan upper ablation site. Although present at a low relative abundance of <1 %, cryoconite from the Himalayas had some microbial functional groups that were not represented in the Antarctic cryoconite. These include functional genes related to methanogenesis, as well as iron and sulfur cycling, i.e., iron respiration, sulfur respiration, sulfate respiration, sulfite respiration, and thiosulfate respiration. In contrast, the functional potential for dark hydrogen oxidation, ureolysis, denitrification, and nitrite respiration was unique to the Antarctic sample and present at a low relative abundance of <1 %.

We also used the Bugbase bioinformatic tool to infer community-wide phenotypes (see supplementary Fig. S2). BugBase identified phenotypes associated with aerobic, anaerobic, facultatively anaerobic, stress tolerance, mobile element, biofilms formation, gram-negative bacteria, and gram-positive bacteria were not significantly different between sites within each geographical location and also between Antarctica and Himalaya (Mann-Whitney-Wilcoxon Test, FDR-corrected  $p$ -value >0.3).

## 4. Discussion

### 4.1. A multi-level trophic organization of the cryoconite hole microbiome

Cyanobacteria were the most abundant bacterial phylum in the Antarctic sites and the lower ablation region of the Himalayas. Cyanobacteria are typically found in glacier ecosystems, especially cryoconite holes (Vincent, 2002). They fix atmospheric nitrogen (Vincent, 2002) and account for 75 and 93 % of the carbon fixation (Stibal and Tranter, 2007), leading to the accumulation of organic matter on glacier surfaces (Anesio et al., 2009). Their secretion of sticky extracellular polymeric substances facilitates the formation of cryoconite granules (Cook et al., 2016), fostering a habitat for a diverse community of heterotrophs (Porazinska et al., 2004). Phototrophic bacteria such as Chloroflexi and eukaryotic phototrophs such as Chlorophyta and Ochrophyta were present at all sites. Chlorophyta and Ochrophyta are common eukaryotic groups in cryoconite holes (Sommers et al., 2018; Lutz et al., 2019; Sommers et al., 2020). Chloroflexi is prevalent in both glacial soil environments and cryoconite as well as on glacier surfaces (Yang et al., 2016; Liu et al., 2017; Millar et al., 2021; Winkel et al., 2022). Together, these primary producers could be responsible for accumulating organic matter within cryoconite holes, as evidenced by significant rates of primary production in these systems (Anesio et al., 2010; Samui et al., 2020).

Proteobacteria, Bacteroidetes, Acidobacteria, Actinobacteria, Verrucomicrobia, Armatimonadetes, and Firmicutes, were present across all sites and are found in glaciers worldwide (Edwards et al., 2013; Cameron et al., 2015; Liu et al., 2017; Sommers et al., 2018; Rathore et al., 2022; Winkel et al., 2022). Additionally, fungi from Ascomycota, Basidiomycota, Blastocladiomycota, Chytridiomycota, and Monoblepharomycota were identified. These taxa are prevalent in Antarctic lakes (Rojas-Jimenez et al., 2017) and glacier surfaces (Rathore et al., 2022; Bradley et al., 2022; Winkel et al., 2022). These heterotrophic bacteria and fungi likely rely on organic carbon from photosynthesis, contributing to carbon flow and nutrient cycling within cryoconite holes (Sanyal et al., 2018, 2020). The archaea Halobacteriaceae, which can degrade diverse carbon compounds, may also contribute to these processes (Andrei et al., 2012). They have been previously associated with Antarctic sea-ice communities (Cowie et al., 2011; Jifei et al., 2014) and coastal Antarctic snowpacks (Antony et al., 2016). Some of the degraded by-products may be utilized by methanogenic Archaea such as *Methanoregulaceae* (Oren, 2014) and *Methanomassiliicoccaceae* (Iino et al., 2013) inhabiting anoxic microzones within the cryoconite (Poniecka et al., 2018; Segawa et al., 2020), to produce methane. Others like Nitrososphaerales, contribute to nitrogen cycling processes (Tournay et al., 2011; Zarsky et al., 2013; Stieglmeier et al., 2014). Thus, several prokaryotic microbial communities co-exist through interactions such as syntrophy and



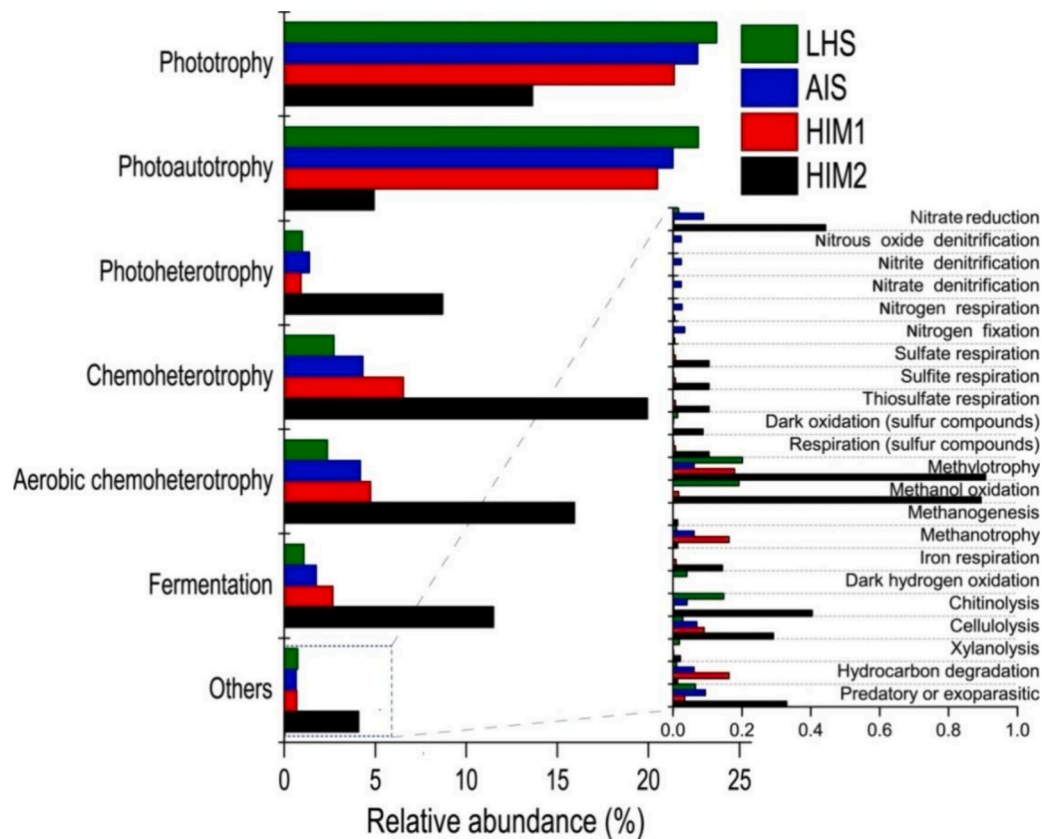


Fig. 4. Predicted bacterial biogeochemical functions based on the FAPROTAX database.

commensalism within the cryoconite microenvironment (Pittino et al., 2023).

Cryoconite also hosts a diversity of heterotrophic eukaryotes including ciliates, cercozoa, rotifers, and tardigrades. Ciliates and cercozoa found worldwide in cryoconite holes (Kaczmarek et al., 2016; Sommers et al., 2018; Lutz et al., 2019), serve as essential links in the food web by feeding on bacteria and microalgae (Porazinska et al., 2004; Mieczan et al., 2013) and serving as a food source for higher trophic levels (Pierce and Turner, 1992). Rotifers (Bdelloidea) were detected at all sites, with higher abundances in the Antarctic cryoconite holes. Bdelloid rotifers could play an important role in the food web by feeding on particulate organic matter, bacteria, yeasts, algae, and small organisms like ciliates and flagellates (Arndt, 1993), with some rotifers, even feeding on other rotifers (De Smet and van Rompu, 1994). Tardigrades were detected in all sites except LHS. Grazers like Tardigrades and Rotifers have different food requirements, playing diverse roles in a cryoconite trophic network (Jaroměřská et al., 2021). They often co-exist in cryoconite holes, although their distribution varies among glaciers, with one species dominating the other (Zawierucha et al., 2021). Together, these grazer communities act as top predators within the cryoconite ecosystem, possibly influencing, at a multitrophic level, the diversity and density of ciliates, flagellates, algae, yeast, and bacteria inhabiting cryoconite holes (Zawierucha et al., 2016; Ricci and Balsamo, 2000). Additionally, their grazing activities could positively influence community composition and the microbial web by releasing nutrients from grazed cells and making them available to other organisms (Arndt, 1993; Vonnahme et al., 2016). Thus, cryoconite habitats harbor diverse microbial communities organized in a self-sustaining multi-level trophic web. Although the sites studied here feature distinct environmental gradients, the consistent presence of certain bacterial, microalgal, fungal, protist, and metazoan invertebrates across all locations (Table S8) indicates their widespread geographical distribution. This suggests that these microbial taxa are resilient and adaptable to diverse

environmental conditions.

#### 4.2. Functional metabolic potential of cryoconite communities

##### 4.2.1. Methane cycling

Both FAPROTAX and PICRUST predicted the presence of key genes involved in the metabolism of methane (methanotrophy) and other one-carbon compounds (methylotrophy) in all habitats. *Methylibium*, which consumes the single carbon (C1) compound methanol and other complex carbon compounds (Stackebrandt et al., 2009), was detected in all 4 habitats, while *Methylotenera*, which consume methylamine and other multicarbon compounds (Kalyuzhnaya et al., 2012) were observed in both the Himalayan sites. Although direct evidence linking the presence of C1 compounds such as formaldehyde (Preunkert et al., 2015), formate (Samui et al., 2017), and methanesulfonic acid (Antony et al., 2010) in supraglacial environments to methylotroph abundance is lacking, transcriptomic studies suggest the role of *Methylotenera*, in the oxidation of formate and formaldehyde (Kalyuzhnaya et al., 2010).

Methanotrophic bacteria from the family Methylocystaceae that utilize methane and methanol as carbon and energy sources were found in all the samples (Bowman, 2006). Methanotrophs often co-occur with non-methane-utilizing methylotrophs, especially *Methylotenera* (Beck et al., 2013; Oshkin et al., 2015; Crevecoeur et al., 2015). This partnership involves the release of methanol by the methanotrophs (during the oxidation of methane), which in turn is consumed by the methylotrophs (Beck et al., 2013; Oshkin et al., 2015). This is consistent with the detection of methanol oxidation potential in the samples. Methanotrophs also commonly co-occur with non-methylotrophic bacteria, most prominently the taxa Burkholderiales, *Flavobacterium*, and *Pseudomonas* (Beck et al., 2013; Oshkin et al., 2015), that feed on organic compounds and exopolymeric substances released by the methanotrophs (Yu and Chistoserdova, 2017). These community partnerships suggest that methanotrophs regulate the methane cycle and serve as important

components of the microbial food web by providing methane-derived organic carbon to other microbial groups.

Microbial production of methane (or methanogenesis) in the Himalayan cryoconite, especially in the upper ablation zone, as determined by FAPROTAX analysis, may be facilitated by anoxic zones within cryoconite deposits (Poniecka et al., 2018; Segawa et al., 2020). Although surface features, cryoconite holes connect to the subglacial environment, delivering meltwater through crevasses and moulins (Fountain et al., 2004; MacDonell et al., 2016). Cryoconite methanogenic archaea, such as *Methanoregulaceae* and *Methanomassiliococcaceae*, detected here and in other studies (Pittino et al., 2023), that is adapted to subglacial conditions, may contribute to anaerobic organic matter turnover upon reaching the subglacial zone (Zdanowski et al., 2017). Methanogens utilize carbon dioxide, hydrogen, acetate, or methylated compounds to produce methane, often in association with bacteria and fungi that produce these compounds during organic matter degradation (Jackson and McInerney, 2002; Evans et al., 2019). This cooperative relationship enhances the efficiency of organic matter breakdown, benefiting associated microbial partners, including methanotrophs, which utilize the methane produced. These dynamics may play a crucial role in regulating methane cycling within cryoconite habitats on glacier surfaces.

#### 4.2.2. Iron cycling

FAPROTAX predictions of iron respiration in cryoconite granules align with the detection of microbes engaged in both iron oxidation and reduction reactions. Key ferric iron reducers *Rhodoferrax*, *Geobacter*, and *Acidiphilium* that convert ferric [Fe(III)] to ferrous [Fe(II)] iron (Kusel et al., 1999; Finneran et al., 2003; Holmes et al., 2007; Coupland and Johnson, 2008) were identified in this study. While *Rhodoferrax* was present in Antarctic and Himalayan cryoconite, *Geobacter* and *Acidiphilium* were exclusively found in the Himalayan samples, suggesting region-specific microbial adaptations influencing iron cycling dynamics. Members of the Comamonadaceae family are capable of iron reduction coupled with anaerobic oxidation of ammonium (Emerson et al., 2015; Bao and Li, 2017). Comamonadaceae were found across all sites, consistent with the prediction of iron-reducing metabolism. The sulfate reducer *Desulfosporosinus*, known for ferric iron reduction (Pester et al., 2012), was present in both Himalayan sites. Given the abundance of iron in cryoconite holes (Singh et al., 2017a; Fortner and Lyons, 2018), iron-reducing bacteria potentially influence sediment geochemistry by driving chemical weathering, contributing to organic matter oxidation, and ion mobilization or immobilization (Weber et al., 2006). Hydrological systems facilitate the transportation of these chemolithoautotrophic microbes from the ice surface to the subglacial system, where oxidized forms of iron are available. Some microbes, such as *Rhodoferrax*, *Geobacter*, and *Desulfosporosinus*, are implicated in iron reduction in subglacial environments (Nixon et al., 2017).

Iron oxidizers like *Rhodobacter* (family Rhodobacteraceae) and *Thiobacillus* (now *Acidithiobacillus*) are prominent in these ecosystems. Rhodobacteraceae are phototrophic iron oxidizers, utilizing soluble ferrous iron and minerals like ferrous sulfide or ferrous carbonate as reductant sources. *Rhodobacter* spp. oxidize iron under circum-neutral pH in micro-aerobic and anaerobic environments, forming iron-rich minerals (Miot et al., 2009; Emerson et al., 2010). These minerals precipitate on extracellular polymeric substances outside the cell, effectively adsorbing metals, phosphates, and dissolved organic matter from the environment (Miot et al., 2009; Bennett et al., 2014). The sulfur-oxidizing bacteria *Thiobacillus*, oxidizes ferrous iron (Hedrich et al., 2011), while fixing carbon dioxide or nitrogen, and can grow autotrophically (Levicán et al., 2008). EPS production aids attachment to metal sulfides (Gehrke et al., 1998) and complexation with ferrous and ferric ions (Tapia et al., 2013), potentially increasing bioleaching rates. Some *Thiobacillus* species use iron sulfide minerals for energy, contributing to mineral solubilization and iron regeneration (Holmes and Bonnefoy, 2007), impacting iron-sulfur mineral weathering in glaciers (Borin et al., 2010). While cyanobacteria and algae dominate primary production in

cryoconite, ferrous iron-fueled chemolithoautotrophs likely contribute significantly to biogeochemical cycling. Iron respiration may enhance organic carbon biomineralization and community respiration. Moreover, biogenic iron oxides offer a reactive surface for the sorption of organic matter, metals, and phosphorus, intricately linking iron cycling to broader biogeochemical processes.

#### 4.2.3. Sulfur cycling

Sulfur cycling in polar regions is relatively understudied, despite the detection of sulfur metabolism genes in cryoconite holes (Edwards et al., 2013; Rathore et al., 2022; Pittino et al., 2023) and glacier ice (Simon et al., 2009; Rathore et al., 2022). Here, pathways for elemental sulfur and inorganic sulfur compound respiration, including sulfate, sulfite, thiosulfate, and sulfide, were identified in Himalayan cryoconite (Fig. 4). *Geobacter*, *Desulfosporosinus*, and *Desulfobulbus* capable of sulfur reduction (Rabus et al., 2013), were identified in the Himalayan sites. *Desulfosporosinus* performs sulfate (Zdanowski et al., 2017) and thio-sulfate reduction alongside organic matter oxidation (Rabus et al., 2013). *Desulfobulbus* under anoxic conditions reduces sulfate, sulfite, and thiosulfate (Rabus et al., 2013), and in the presence of oxygen, oxidizes sulfide, elemental sulfur, and sulfite to sulfate (Fuseler and Cypionka, 1995). Although functional pathways related to the sulfur cycle were not predicted in the Antarctic samples, the presence of *Desulfobulbus* in AIS and sulfur-oxidizing bacteria *Thiobacillus* (Heddrich et al., 1998) in LHS implies potential sulfur cycling in these environments. Sulfate reduction to sulfide, via diverse sulfur intermediates, plays a crucial role in mineralizing sediment organic matter in cold regions (Sørensen et al., 2015), and is tightly linked with carbon cycling. Hydrogen sulfide and other reduced sulfur intermediates can be abiotically oxidized or serve as electron donors for sulfur-oxidizing microorganisms, leading to the re-oxidation of sulfide to sulfate using oxidants such as oxygen, nitrate, manganese, and iron (Rickard, 2012). Thus, sulfur cycling is closely linked with the cycling of carbon and other elements like nitrogen, manganese, and iron, with implications for both cellular- and ecosystem-level processes on the glacier surface. The high potential for sulfur cycling in the Himalayan region, especially in the upper ablation zone, compared to the Antarctic, may be due to the high content of sulfate ions and sulfur-bearing minerals in the Himalayan glaciers (Singh et al., 2017b). Sulfur-oxidizing bacteria commonly colonize carbonate minerals and catalyze their dissolution through hydrogen ion production (Leprich et al., 2021). Thus, sulfur-oxidizing activities could impact the lithotrophic dissolution of carbonate minerals on the glacier surface.

#### 4.2.4. Nitrogen cycling

Supraglacial cryoconite communities have been observed to facilitate essential transformations within the nitrogen cycle (Telling et al., 2011; Cameron et al., 2012; Segawa et al., 2014). While nifH genes detected in cryoconite did not match those in the database, FAPROTAX predictions confirmed the potential for atmospheric nitrogen fixation. This potential appeared slightly higher in the LHS region, likely influenced by low NO<sub>3</sub><sup>-</sup> levels in samples from this site. Given the energy-intensive nature of nitrogen fixation, its regulation aligns closely with the availability of environmental ammonium (Dixon and Kahn, 2004). Hence, microbes in glaciers receiving minimal NO<sub>3</sub><sup>-</sup> inputs may rely on atmospheric nitrogen fixation to meet their nitrogen requirements, while those with higher NO<sub>3</sub><sup>-</sup> inputs likely adjust nitrogen fixation in response to environmental cues. Nitrogen fixation is a crucial source of assimilatory nitrogen for resident microbes when alternative nitrogen sources, such as snow and ice melt, become limited (Telling et al., 2011). Previous studies have provided evidence for nitrogen fixation within cryoconite sediment through functional marker gene analysis (Segawa et al., 2014), functional predictions (Rathore et al., 2022), isotope studies (Segawa et al., 2014), and in situ laboratory assays (Telling et al., 2011).

We identified nitrifier communities by investigating bacterial and



archaeal ammonia monooxygenase (AmoA) genes, catalyzing the initial step of nitrification, i.e., ammonia oxidation. While some studies reported low relevance of ammonia oxidation and nitrification in cryoconite (Pittino et al., 2023), our findings align with others detecting the genetic potential for nitrification in microbial communities within cryoconite granules (Cameron et al., 2012; Segawa et al., 2014). Nitrification is thought to increase nitrate concentrations within cryoconite holes (Bagshaw et al., 2013), playing a pivotal role in the nitrogen cycle by regulating the availability of ammonium and nitrate.

Bacteria-specific AmoA gene sequenced from AIS in Antarctica showed similarity to the AmoA gene from *Nitrosospira*, consistent with previous findings (Segawa et al., 2014). *Nitrosospira* uniquely performs both steps of nitrification converting ammonia to nitrite and then nitrite to nitrate. This complete nitrification process is energetically favorable compared to individual steps, potentially giving *Nitrosospira* a growth advantage over organisms performing either of the single steps of nitrification alone (Daims et al., 2015).

The archaea-specific AmoA gene associated with Crenarchaeota was detected and amplified from AIS, suggesting a potential contribution of archaea to ammonia oxidation within cryoconite. While the archaeal AmoA gene was not amplified from Himalayan cryoconite, the presence of ammonia-oxidizing archaea *Nitrososphaerales* (Crenarchaeota) (Tourna et al., 2011; Zarsky et al., 2013; Stieglmeier et al., 2014) in the upper ablation zone implies their involvement in nitrogen cycling in this region. Ammonia-oxidizing Crenarchaeota is abundant in soil ecosystems, influencing nitrogen biogeochemical transformations (Leininger et al., 2006). These nitrifier communities could be supported by the availability of ammonium ions in the Himalayan cryoconite (Table 1).

In the environment, denitrification accounts for a significant reduction of inorganic nitrogen to nitrous oxide or nitrogen gas through several steps. FAPROTAX analysis indicated the potential for nitrate reduction in all sites except the lower ablation region in the Himalayas. However, amplification of the nitrate reductase gene *narG*, responsible for catalyzing nitrate reduction to nitrite, was observed in the lower ablation site, indicating the presence of nitrate reducers within cryoconite granules. The potential nitrate reducers found could not be classified into any specific phylogenetic group, as they are closely related to uncultured bacterial clones. FAPROTAX predictions indicated the potential for the complete denitrification pathway, involving nitrate reduction to nitrogen gas, in AIS. The nitrous oxide reductase gene (*nosZ*), responsible for converting nitrous oxide to nitrogen gas, identified in both Himalayan sites, was associated with *nosZ* sequences from Rhizobiales, which are predominant nitrous oxide reducers in glacier soils (Zeng et al., 2016). These findings suggest the presence of genes encoding enzymes for denitrification within cryoconite, consistent with metatranscriptomic studies where the genes for the complete denitrification pathway have been transcribed from cryoconite (Pittino et al., 2023). The detection of nitrogen fixation, nitrification, and denitrification genes suggests the co-existence of nitrogen fixers, nitrifiers, and denitrifiers within cryoconite granules, possibly supported by the fine-scale redox stratification within these granules (Poniecka et al., 2018; Segawa et al., 2020). PICRUSt analysis further confirmed the genetic potential for nitrogen metabolism across all sites (Fig. 3).

#### 4.2.5. Carbon cycling

The presence of the *rbcl* gene responsible for carbon fixation within the Stramenopiles, Synechococcales, Oscillatoriales, Chromatiales, and the *cbbLR* gene within the Rhizobiales and Burkholderiales is consistent with the identification of these taxa (except Chromatiales) through the 16S/18S rRNA gene analysis. These findings are similar to those of Cameron et al. (2012), where functional genes associated with carbon cycling were observed in cryoconite granules. The potential for carbon cycling has also been observed in other Himalayan sites (Rathore et al., 2022).

Functional FAPROTAX predictions indicate significant photoautotrophic activity in cryoconite, with cyanobacterial abundances and

carbon fixation genes prevalent across sites, except the upper ablation site in the Himalayas. This aligns with previous research suggesting lower cyanobacterial abundance at higher elevations (Segawa et al., 2014), potentially affecting carbon cycling (Segawa et al., 2020). However, recent findings show higher phototroph abundance and productivity at higher elevations (Shamurailatpam et al., 2023), attributed to factors like greater light availability, thin sediment thickness (< 3 cm), smaller grain size of the cryoconite mineral particles, and greater stability of cryoconite holes (Shamurailatpam et al., 2023). Sediment thickness and grain size were not measured in our study, limiting the assessment of their impact on autotroph abundance and carbon fixation (Shamurailatpam et al., 2023). Solar radiation, particularly photosynthetically active radiation (PAR), regulates photosynthesis and primary production and is influenced by topographic shading (Olson and Rupper, 2019). While PAR was not directly measured in our study, it is unlikely to be significantly impacted by local topographical shading given that the Himalayan glacier is east-facing. In addition to cyanobacteria, Proteobacteria also harbor *rbcl* genes and could substantially contribute to CO<sub>2</sub> fixation in cryoconite holes (Franzetti et al., 2016), indicating widespread carbon fixation potential. However, variables like altitude, sunlight availability, cryoconite thickness, and grain size likely regulate their activity (Langford et al., 2014; Chandler et al., 2015; Shamurailatpam et al., 2023). We acknowledge the limitations of not considering these factors in our study, which constrain data interpretation.

Himalayan cryoconite exhibited higher heterotrophic activity and carbon degradation potential compared to Antarctic cryoconite, likely due to increased organic matter availability from external sources such as mineral dust and biomass-burning products (Stibal et al., 2008; Xu et al., 2010; Nizam et al., 2020; Xu et al., 2013). The total organic carbon concentration in the Himalayan cryoconite holes was 1 to 2 orders higher than that in the Antarctic (Table 1; Sanyal et al., 2018), a significant fraction of which is bioavailable (Sanyal et al., 2018). In contrast, in Antarctica, external sources of organic matter may be limited, especially in open cryoconite holes, while in-situ production could be prevalent (Samui et al., 2020).

Multiple genera across the phyla Proteobacteria, Bacteroidetes, Firmicutes, Basidiomycota, and Actinobacteria identified in the present study have been previously isolated from these Antarctic and Himalayan cryoconite holes (Sanyal et al., 2018, 2020). These microbes utilize various organic compounds such as plant polysaccharides, carbohydrates, proteins, and lipids (Sanyal et al., 2018, 2020) that are prevalent in these environments (Pautler et al., 2013; Feng et al., 2016). These results are consistent with the key functions for carbohydrate, amino acid, and lipid metabolism predicted through PICRUSt analysis, suggesting that the carbon degradation potential of the microbial community is closely associated with the composition of available organic compounds. Overall, our findings are consistent with studies that show that carbon is fixed and cycled within this ecosystem through photosynthesis, respiration (Anesio et al., 2010; Telling et al., 2010; Cook et al., 2012), and organic carbon uptake (Sanyal et al., 2018).

Our study provides valuable insights into cryoconite ecology across glaciers with different environmental conditions. However, we acknowledge that the small sample size and the absence of hypothesis-driven experimental manipulations limit our ability to draw definitive conclusions about the relationships between environmental factors and microbial communities. Furthermore, our snapshot sampling approach may not fully capture the spatial and temporal variability inherent in glacier ecosystems. Future research employing hypothesis-driven methodologies and larger sample sizes is warranted to address these limitations and advance the field.

## 5. Conclusions

Cryoconite holes are highly structured, small-scale ecosystems, at the base of which are microalgae, cyanobacteria, and chemoautotrophic

bacteria, which, through primary production, enrich the cryoconite with organic matter. This organic matter supports a complex, multi-layered microbial ecosystem that comprises heterotrophic bacteria, archaea, fungi, and a variety of microfauna, including protozoans, ciliates, rotifers, and tardigrades. These organisms contribute to the decomposition and mineralization of organic material and the recycling of nutrients in cryoconite holes. While certain microbial taxa were found ubiquitously across all sites, distinct regional adaptations in microbial diversity and biogeochemical potentials were evident, corresponding to the unique environmental conditions in the Antarctic and Himalayan glaciers. The diversity and genetic potential of the cryoconite microbial community observed on the different glaciers hint at the capability of cryoconite communities to carry out complete cycling of essential elements such as carbon, nitrogen, sulfur, and/or iron (Fig. 5). For example, through functional predictions using 16S rRNA gene sequence and analysis of marker genes involved in various aspects of the nitrogen cycle, we find that the potential to perform complete nitrogen cycle exists at AIS. The AIS cryoconite community was capable of fixing atmospheric nitrogen, oxidizing ammonia, and carrying out the complete denitrification pathway of nitrate reduction to nitrogen gas. The capability for complete iron cycling through iron oxidation and reduction reactions was noted in all samples through FAPROTAX analysis and the detection of iron reducers like *Rhodospirillum rubrum*, *Geobacter*, and *Acidiphilium* and iron oxidizers like *Rhodospirillum rubrum* and *Thiobacillus*. Methanogenic archaea (Methanoregulaceae and Methanomassiliococcaceae) that produce methane during organic matter decomposition and methanotrophic bacteria (Methylocystaceae) that utilize methane as carbon and energy sources

were found to co-exist in the Himalayan region. This suggests that these environments provide niches that support the complete cycling of methane. FAPROTAX predictions were congruent with detecting microbes involved in both the production and consumption of methane. Similarly, the detection of pathways related to the respiration of elemental sulfur and inorganic sulfur compounds such as sulfate, sulfite, thiosulfate, and sulfide in the Himalayan cryoconite indicate that a complete sulfur cycle may be functioning within these communities. The co-presence of sulfur reducers *Geobacter*, *Desulfosporosinus*, *Desulfobulbus*, and the sulfur oxidizer *Thiobacillus* supports this. Taken as a whole, it is apparent that cryoconite holes comprise a closely-knit community of remarkably diverse and complex functional phylotypes that link all of Earth's important biogeochemical cycles. Moreover, the photoautotrophic and chemolithotrophic communities within these cryoconite holes might provide a source of carbon, nitrogen, sulfur, and iron to the surrounding ecosystems when flushing events transport cryoconite material via meltwater to streams, soils, lakes, rivers, oceans, etc., thereby sustaining downstream glacier and aquatic food webs. Cryoconite hole organic matter can also be transported via the englacial hydrological system down to subglacial environments, fuelling microbial processes in subglacial systems. This is important in the context of increased glacier retreat and melting of vast expanses of the glacier surface, which results in changes in surface hydrology. While the data gathered here reflects potential rather than realized functional capacity, it provides crucial insights on microbially driven transformations of carbon, nitrogen, sulfur, and iron in cryoconite ecosystems that underpin an important mechanism for delivering nutrients to downstream

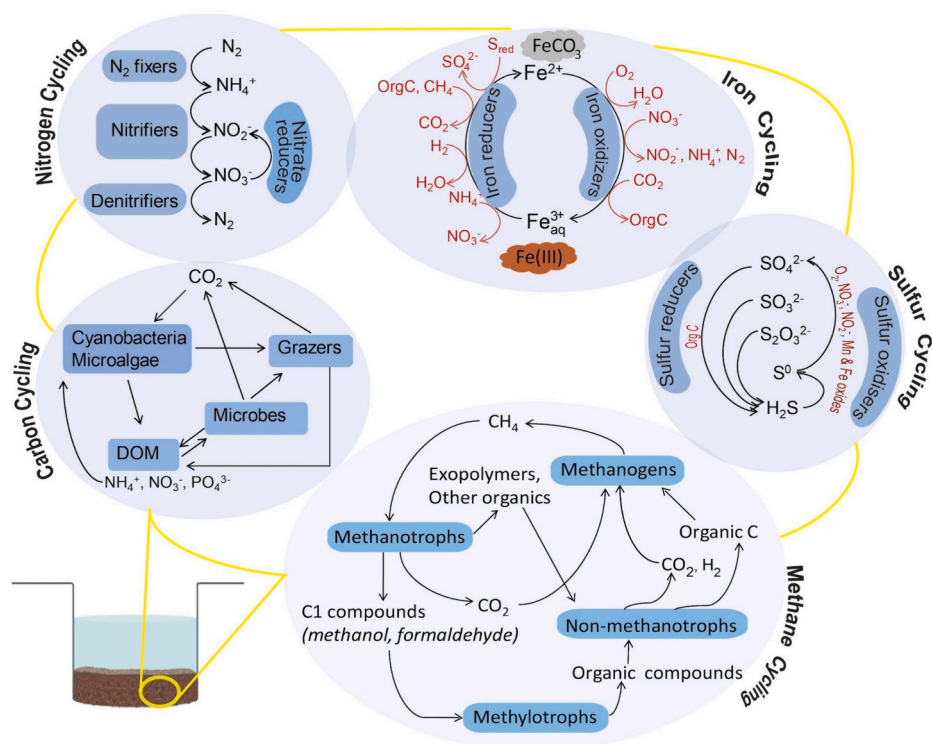


**Fig. 5.** Schematic overview of potential transformations of crucial elements by cryoconite microbial communities (1) Carbon Cycle: Cyanobacteria and microalgae fix atmospheric carbon dioxide ( $\text{CO}_2$ ) to organic carbon. This organic carbon supports heterotrophic microbes and meiofauna which in turn contribute to the decomposition and mineralization of organic material and recycling of nutrients; (2) Nitrogen Cycle: Atmospheric nitrogen fixed by microbes is metabolized to nitrite ( $\text{NO}_2^-$ ), nitrate ( $\text{NO}_3^-$ ), and nitrogen gas ( $\text{N}_2$ ) through nitrification and denitrification; (3) Iron Cycle: Iron reducers reduce aqueous or mineral phase ferric iron ( $\text{Fe}^{3+}$ ) coupled to the oxidation of organic carbon (OrgC), reduced sulfur ( $\text{S}_{\text{red}}$ ) and ammonium ( $\text{NH}_4^+$ ). Iron oxidizers oxidize ferrous iron ( $\text{Fe}^{2+}$ ) with oxygen, nitrate, or bicarbonate (via photosynthesis) as electron acceptor; (4) Sulfur Cycle: Microbial reduction of sulfate to sulfide via diverse sulfur intermediates facilitates the mineralization of organic matter. Hydrogen sulfide and elemental sulfur are re-oxidized to sulfate by sulfur-oxidizing microbes through reactions that involve oxidants such as oxygen, nitrate, manganese, and iron; (5) Methane Cycle: Methanogenic archaea convert carbon dioxide and hydrogen, acetate, or methylated compounds to methane, in association with bacteria and fungi that produce these compounds. Methanotrophic bacteria utilize this methane and release methanol, organic acids, and polymeric substances that are consumed by methylotrophs and non-methylotrophic bacteria.

ecosystems. Further research is necessary to explore the effect of environmental factors on the functioning of these simple but closely-knit ecosystems. As such, it is important to know how microbial carbon and nutrient cycles respond to ongoing and future climate scenarios.

### CRedit authorship contribution statement

**Runa Antony:** Writing – original draft, Investigation, Formal analysis, Conceptualization. **Dattatray Mongad:** Validation, Software, Data curation. **Aritri Sanyal:** Methodology, Investigation, Formal analysis. **Dhiraj Dhotre:** Validation, Resources. **Meloth Thamban:** Resources, Funding acquisition.

### Declaration of competing interest

The authors declare that they have no known competing financial interests or personal relationships that could have appeared to influence the work reported in this paper.

### Data availability

Data has been shared in the supplementary file.

### Acknowledgments

We thank Ashish Paiguinkar for assistance with ion chromatography analysis and sample collection from Himalaya, Lavkush Patel for field assistance in Himalaya, and Shunan Feng for preparing the map. RA thanks the European Research Council (ERC) Synergy Grant DEEP PURPLE under the European Union's Horizon 2020 research and innovation program (grant agreement No 856416) for supporting her research stay in Germany. This study was funded by the Ministry of Earth Sciences under the PACER-Cryosphere and Climate project. This is NCPOR contribution number J-5/2024-25.

### Appendix A. Supplementary data

Supplementary data to this article can be found online at <https://doi.org/10.1016/j.scitotenv.2024.173187>.

### References

- Andrei, A.S., Banciu, H.L., Oren, A., 2012. Living with salt: metabolic and phylogenetic diversity of archaea inhabiting saline ecosystems. *FEMS Microbiol. Lett.* 330 (1), 1–9. <https://doi.org/10.1111/j.1574-6968.2012.02526.x>.
- Anesio, A.M., Hodson, A., Fritz, A., Psenner, R., Sattler, B., 2009. High microbial activity on glacier: importance to the global carbon cycle. *Glob. Chang. Biol.* 15, 955–960. <https://doi.org/10.1111/j.1365-2486.2008.01758.x>.
- Anesio, A.M., Sattler, B., Foreman, C., Telling, J., Hodson, A., Tranter, M., Psenner, R., 2010. Carbon fluxes through bacterial communities on glacier surfaces. *Ann. Glaciol.* 51 (56), 32–40. <https://doi.org/10.3189/172756411795932092>.
- Antony, R., Thamban, M., Krishnan, K.P., Mahalinganathan, K., 2010. Is cloud seeding in coastal Antarctica linked to bromine and nitrate variability in snow? *Environ. Res. Lett.* <https://doi.org/10.1088/1748-9326/5/1/014009>.
- Antony, R., Mahalinganathan, K., Thamban, M., Nair, S., 2011. Organic carbon in Antarctic snow: Spatial trends and possible sources. *Environ. Sci. Technol.* 45 (23), 9944–9950. <https://doi.org/10.1021/es203512t>.
- Antony, R., Sanyal, A., Kapse, N., Dhakephalkar, P.K., Thamban, M., Nair, S., 2016. Microbial communities associated with Antarctic snow pack and their biogeochemical implications. *Microbiol. Res.* 192, 192–202. <https://doi.org/10.1016/j.micres.2016.07.004>.
- Arndt, H., 1993. Rotifers as predators on components of the microbial web (bacteria, heterotrophic flagellates, ciliates)—a review. In *Rotifer Symposium VI: Proceedings of the Sixth International Rotifer Symposium, held in Banyoles, Spain, June 3–8, 1991* (pp. 231–246). Springer Netherlands. doi:<https://doi.org/10.1007/bf00025844>.
- Baccolo, G., Di Mauro, B., Massabò, D., Clemenza, M., Nastasi, M., Delmonte, B., Prata, M., Prati, P., Previtali, E., Maggi, V., 2017. Cryoconite as a temporary sink for anthropogenic species stored in glaciers. *Sci. Rep.* 7 (1), 9623. <https://doi.org/10.1038/s41598-017-10220-5>.
- Bagshaw, E.A., Tranter, M., Fountain, A.G., Welch, K., Basagic, H.J., Lyons, W.B., 2013. Do cryoconite holes have the potential to be significant sources of C, N, and P to downstream depauperate ecosystems of Taylor Valley, Antarctica? *Arct. Antarct. Alp. Res.* 45 (4), 440–454. <https://doi.org/10.1657/1938-4246-45.4.440>.
- Bao, P., Li, G.X., 2017. Sulfur-driven iron reduction coupled to anaerobic ammonium oxidation. *Environ. Sci. Technol.* 51 (12), 6691–6698. <https://doi.org/10.1021/acs.est.6b05971>.
- Beck, D.A., Kalyuzhnaya, M.G., Malfatti, S., Tringe, S.G., Del Río, T.G., Ivanova, N., Lidstrom, M.E., Chistoserdova, L., 2013. A metagenomic insight into freshwater methane-utilizing communities and evidence for cooperation between the Methylococaceae and the Methylophilaceae. *PeerJ* 1, e23. <https://doi.org/10.7717/peerj.23>.
- Bennett, S.A., Toner, B.M., Barco, R., Edwards, K.J., 2014. Carbon adsorption onto Fe oxyhydroxide stalks produced by lithotrophic iron-oxidizing bacteria. *Geomicrobiol. J.* 12 (2), 146–156. <https://doi.org/10.1111/gbi.12074>.
- Bookhagen, B., Burbank, D.W., 2010. Toward a complete Himalayan hydrological budget: spatiotemporal 780 distribution of snowmelt and rainfall and their impact on river discharge. *Case Rep. Med.* 115 (3), 1–25. <https://doi.org/10.1029/2009JF001426>.
- Borin, S., Ventura, S., Tambone, F., Mapelli, F., Schubotz, F., Brusetti, L., Scaglia, B., D'Acqui, L.P., Solheim, B., Turicchia, S., Marasco, R., 2010. Rock weathering creates oases of life in a high Arctic desert. *Environ. Microbiol.* 12 (2), 293–303. <https://doi.org/10.1111/j.1462-2920.2009.02059.x>.
- Bowman, J., 2006. The methanotrophs—the families Methylococaceae and Methylocystaceae. *The. prokaryotes* 5, 266–289. [https://doi.org/10.1007/0-387-30745-1\\_15](https://doi.org/10.1007/0-387-30745-1_15).
- Bradley, J.A., Trivedi, C.B., Winkel, M., Mouro, R., Lutz, S., Larose, C., Keusch, C., Doting, E., Halbach, L., Zervas, A., Anesio, A.M., Benning, L.G., 2022. Active and dormant microorganisms on glacier surfaces. *Geobiology* 21 (2), 244–261. <https://doi.org/10.1111/gbi.12535>.
- Cameron, K.A., Hodson, A.J., Osborn, A.M., 2012. Carbon and nitrogen biogeochemical cycling potentials of supraglacial cryoconite communities. *Polar Biol.* 35, 1375–1393. <https://doi.org/10.1007/s00300-012-1178-3>.
- Cameron, K.A., Hagedorn, B., Diesler, M., Christner, B.C., Choquette, K., Sletten, R., Crump, B., Kellogg, C., Junge, K., 2015. Diversity and potential sources of microbiota associated with snow on western portions of the Greenland ice sheet. *Environ. Microbiol.* 17 (3), 594–609. <https://doi.org/10.1111/1462-2920.12446>.
- Caporaso, J.G., Lauber, C.L., Walters, W.A., Berg-Lyons, D., Huntley, J., Fierer, N., Owens, S.M., Betley, J., Fraser, L., Bauer, M., Gormley, N., 2012. Ultra-high-throughput microbial community analysis on the Illumina HiSeq and MiSeq platforms. *ISME J.* 6 (8), 1621–1624. <https://doi.org/10.1038/ismej.2012.8>.
- Chandler, D.M., Alcock, J.D., Wadham, J.L., Mackie, S.L., Telling, J., 2015. Seasonal changes of ice surface characteristics and productivity in the ablation zone of the Greenland ice sheet. *Cryosphere* 9, 487–504. <https://doi.org/10.5194/tc-9-487-2015>.
- Cook, J., Edwards, A., Takeuchi, N., Irvine-Fynn, T., 2016. Cryoconite: the dark biological secret of the cryosphere. *Prog. Phys. Geogr.* 40 (1), 66–111. <https://doi.org/10.1177/0309133315616574>.
- Cook, J.M., Hodson, A.J., Anesio, A.M., Hanna, E., Yallop, M., Stibal, M., Telling, J., Huybrechts, P., 2012. An improved estimate of microbially mediated carbon fluxes from the Greenland ice sheet. *J. Glaciol.* 58 (212), 1098–1108. <https://doi.org/10.3189/2012JoG12J001>.
- Coupland, K., Johnson, D.B., 2008. Evidence that the potential for dissimilatory ferric iron reduction is widespread among acidophilic heterotrophic bacteria. *FEMS Microbiol. Lett.* 279 (1), 30–35. <https://doi.org/10.1111/j.1574-6968.2007.00998.x>.
- Cowie, R.O.M., Mass, E.W., Ryan, K.G., 2011. Archaeal diversity revealed in Antarctic Sea ice. *Antarct. Sci.* 23, 531–536.
- Crevecoeur, S., Vincent, W.F., Comte, J., Lovejoy, C., 2015. Bacterial community structure across environmental gradients in permafrost thaw ponds: methanotrophic ecosystems. *Front. Microbiol.* 6, 192. <https://doi.org/10.3389/fmicb.2015.00192>.
- Daims, H., Lebedeva, E.V., Pjevac, P., Han, P., Herbold, C., Albertsen, M., Jehmlich, N., Palatinszky, M., Vierheilig, J., Bulaev, A., Kirkegaard, R.H., 2015. Complete nitrification by *Nitrosipira* bacteria. *Nature* 528 (7583), 504–509. <https://doi.org/10.1038/nature16461>.
- De Smet, W.H., Van Rompu, E.A., 1994. Rotifera and Tardigrada from cryoconite holes on a Spitsbergen (Svalbard) glacier. *Belg. J. Zool.* 124, 27–37.
- Di Mauro, B., Baccolo, G., Garzonio, R., Giardino, C., Massabò, D., Piazzalunga, A., Rossini, M., Colombo, R., 2017. Impact of impurities and cryoconite on the optical properties of the Morteratsch glacier (Swiss Alps). *Cryosphere* 11 (6), 2393–2409. <https://doi.org/10.5194/tc-11-2393-2017>.
- Dixon, R., Kahn, D., 2004. Genetic regulation of biological nitrogen fixation. *Nat. Rev. Microbiol.* 2 (8), 621–631. <https://doi.org/10.1038/nrmicro954>.
- Edwards, A., Pachebat, J.A., Swain, M., Hegarty, M., Hodson, A.J., Irvine-Fynn, T.D., Rassner, S.M., Sattler, B., 2013. A metagenomic snapshot of taxonomic and functional diversity in an alpine glacier cryoconite ecosystem. *Environ. Res. Lett.* 8 (3), 035003. <https://doi.org/10.1088/1748-9326/8/3/035003>.
- Emerson, D., Fleming, E.J., McBeth, J.M., 2010. Iron-oxidizing bacteria: an environmental and genomic perspective. *Ann. Rev. Microbiol.* 64, 561–583. <https://doi.org/10.1146/annurev.micro.112408.134208>.
- Emerson, D., Scott, J.J., Benes, J., Bowden, W.B., 2015. Microbial iron oxidation in the arctic tundra and its implications for biogeochemical cycling. *Appl. Environ. Microbiol.* 81 (23), 8066–8075. <https://doi.org/10.1128/AEM.02832-15>.
- Evans, P.N., Boyd, J.A., Leu, A.O., Woodcroft, B.J., Parks, D.H., Hugenholz, P., Tyson, G.W., 2019. An evolving view of methane metabolism in the Archæa. *Nat. Rev. Microbiol.* 17 (4), 219–232. <https://doi.org/10.1038/s41579-018-0136-7>.



- Feng, L., Xu, J., Kang, S., Li, X., Li, Y., Jiang, B., Shi, Q., 2016. Chemical composition of microbe-derived dissolved organic matter in cryoconite in Tibetan plateau glaciers: insights from fourier transform ion cyclotron resonance mass spectrometry analysis. *Environ. Sci. Technol.* 50 (24), 13215–13223. <https://doi.org/10.1021/acs.est.6b03971>.
- Finneran, K., Johnsen, C., Lovley, D., 2003. *Rhodoferrax ferrireducens* sp. nov., a psychrotolerant, facultatively anaerobic bacterium that oxidizes acetate with the reduction of Fe(III). *Int. J. Syst. Evol. Microbiol.* 53 (3), 669–673. <https://doi.org/10.1099/ijs.0.02298-0>.
- Fortner, S.K., Lyons, W.B., 2018. Dissolved trace and minor elements in cryoconite holes and supraglacial streams, Canada glacier. *Antarctica. Front. Earth. Sci.* 6 <https://doi.org/10.3389/feart.2018.00031>.
- Fountain, A.G., Tranter, M., Nysten, T.H., Lewis, K.J., Mueller, D.R., 2004. Evolution of cryoconite holes and their contribution to meltwater runoff from glaciers in the McMurdo dry valleys. *Antarctica. J. Glaciol.* 50 (168), 35–45. <https://doi.org/10.3189/172756504781830312>.
- Franzetti, A., Tagliapietra, I., Gandolfi, I., Bestetti, G., Minor, U., Mayer, C., Azzoni, R.S., Diolaiuti, G., Smiraglia, C., Ambrosini, R., 2016. Light-dependent microbial metabolisms drive carbon fluxes on glacier surfaces. *ISME J.* 10 (12), 2984–2988. <https://doi.org/10.1038/ismej.2016.72>.
- Fuseler, K., Cypionka, H., 1995. Elemental sulfur as an intermediate of sulfide oxidation with oxygen by *Desulfobulbus propionicus*. *Arch. Microbiol.* 164, 104–109. <https://doi.org/10.1007/BF02525315>.
- Gehrke, T., Telegdi, J., Thierry, D., Sand, W., 1998. Importance of extracellular polymeric substances from *Thiobacillus ferrooxidans* for bioleaching. *Appl. Environ. Microbiol.* 64 (7), 2743–2747. <https://doi.org/10.1128/AEM.64.7.2743-2747.1998>.
- Hammer-Muntz, O., Harper, D., Ryan, P.D., 2001. *PAST: paleontological statistics software package for education and data analysis version 2.09*.
- Hedderich, R., Klimmek, O., Kröger, A., Dirmeier, R., Keller, M., Stetter, K.O., 1998. Anaerobic respiration with elemental sulfur and with disulfides. *FEMS Microbiol. Rev.* 22 (5), 353–381. <https://doi.org/10.1111/j.1574-6976.1998.tb00376.x>.
- Hedrich, S., Schlömann, M., Johnson, D.B., 2011. The iron-oxidizing proteobacteria. *Microbiology* 157 (6), 1551–1564. <https://doi.org/10.1099/mic.0.045344-0>.
- Hodson, A., Anesio, A.M., Ng, F., Watson, R., Quirk, J., Irvine-Fynn, T., Dye, A., Clark, C., McCloy, P., Kohler, J., Sattler, B., 2007. A glacier respire: quantifying the distribution and respiration CO<sub>2</sub> flux of cryoconite across an entire Arctic supraglacial ecosystem. *Eur. J. Vasc. Endovasc. Surg.* 112 (G4) <https://doi.org/10.1029/2007JG000452>.
- Holmes, D.E., O'Neil, R.A., Vronis, H.A., N'guessan, L.A., Ortiz-Bernad, I., Larrahondo, M.J., Adams, L.A., Ward, J.A., Nicoll, J.S., Nevin, K.P., Chavan, M.A., 2007. Subsurface clade of *Geobacteraceae* that predominates in a diversity of Fe(III)-reducing subsurface environments. *ISME J.* 1 (8), 663–677. <https://doi.org/10.1038/ismej.2007.85>.
- Holmes, D.S., Bonnefoy, V., 2007. Genetic and bioinformatic insights into iron and sulfur oxidation mechanisms of bioleaching organisms. In: Rawlings, D.E., Johnson, D.B. (Eds.), *Biomining*. Springer, Berlin, pp. 281–307. [https://doi.org/10.1007/978-3-540-34911-2\\_14](https://doi.org/10.1007/978-3-540-34911-2_14).
- Iino, T., Tamaki, H., Tamazawa, S., Ueno, Y., Ohkuma, M., Suzuki, K.I., Igarashi, Y., Haruta, S., 2013. Candidatus *Methanogranum caenicola*: a novel methanogen from the anaerobic digested sludge, and proposal of *Methanomassiliicocaceae* fam. Nov. and *Methanomassiliicocales* Ord. Nov., for a methanogenic lineage of the class Thermoplasmata. *Microbes Environ.* 28 (2), 244–250. <https://doi.org/10.1264/jsmc.2.me12189>.
- Jackson, B., McInerney, M., 2002. Anaerobic microbial metabolism can proceed close to thermodynamic limits. *Nature* 415 (6870), 454–456. <https://doi.org/10.1038/415454a>.
- Jaroměřská, T.N., Trubač, J., Zawierucha, K., Vondrovicová, L., Devetter, M., Žárský, J. D., 2021. Stable isotopic composition of top consumers in Arctic cryoconite holes: revealing divergent roles in a supraglacial trophic network. *Biogeosciences* 18, 1543–1557. <https://doi.org/10.5194/bg-18-1543-2021>.
- Jifei, M.A., Zongjun, D.U., Wei, L.U.O., Yong, Y.U., Yixin, Z., Bo, C., Huirong, L.I., 2014. Archaeal diversity and abundance within different layers of summer sea-ice and seawater from Prydz Bay, Antarctica. *Adv. Polar Sci.* 25, 54–60.
- Kaczmarek, L., Jakubowska, N., Celewicz-Goldyn, S., Zawierucha, K., 2016. The microorganisms of cryoconite holes (algae, Archaea, bacteria, cyanobacteria, fungi, and Protista): a review. *Polar Record* 52 (2), 176–203. <https://doi.org/10.1017/S0032247415000637>.
- Kalyuzhnaya, M.G., Beck, D.A., Suci, D., Pozhitkov, A., Lidstrom, M.E., Chistoserdova, L., 2010. Functioning *in situ*: gene expression in *Methylotenera mobilis* in its native environment as assessed through transcriptomics. *ISME J.* 4 (3), 388–398. <https://doi.org/10.1038/ismej.2009.117>.
- Kalyuzhnaya, M.G., Beck, D.A., Vorobev, A., Smalley, N., Kunkel, D.D., Lidstrom, M.E., Chistoserdova, L., 2012. Novel methylotrophic isolates from lake sediment, description of *Methylotenera versatilis* sp. nov. and emended description of the genus *Methylotenera*. *Int. J. Syst. Evol. Microbiol.* 62 (1), 106–111. <https://doi.org/10.1099/ijs.0.029165-0>.
- Kim, M., Jung, J.Y., Laffly, D., Kwon, H.Y., Lee, Y.K., 2017. Shifts in bacterial community structure during succession in a glacier foreland of the high Arctic. *FEMS. Microb. Ecol.* 93 (1), fiw213. <https://doi.org/10.1093/femsec/fiw213>.
- King, M.D., Howat, I.M., Candela, S.G., Noh, M.J., Jeong, S., Noël, B.P., van den Broeke, M.R., Wouters, B., Negrete, A., 2020. Dynamic ice loss from the Greenland ice sheet driven by sustained glacier retreat. *Commun. Earth. Environ.* 1 (1), 1. <https://doi.org/10.1038/s43247-020-0001-2>.
- Kozich, J.J., Westcott, S.L., Baxter, N.T., Highlander, S.K., Schloss, P.D., 2013. Development of a dual-index sequencing strategy and curation pipeline for analyzing amplicon sequence data on the MiSeq Illumina sequencing platform. *Appl. Environ. Microbiol.* 79 (17), 5112–5120. <https://doi.org/10.1128/AEM.01043-13>.
- Kusel, K., Dorsch, T., Acker, G., Stackebrandt, E., 1999. Microbial reduction of Fe(III) in acidic sediments: isolation of *Acidiphilium* cryptum JF-5 capable of coupling the reduction of Fe(III) to the oxidation of glucose. *Appl. Environ. Microbiol.* 65 (8), 3633–3640. <https://doi.org/10.1128/AEM.65.8.3633-3640.1999>.
- Langford, H.J., Irvine-Fynn, T.D.L., Edwards, A., Banwart, S.A., Hodson, A.J., 2014. A spatial investigation of the environmental controls over cryoconite aggregation on Longyearbreen glacier. *Svalbard. Biogeosci.* 11, 5365–5380. <https://doi.org/10.5194/bg-11-5365-2014>.
- Langille, M.G., Zaneveld, J., Caporaso, J.G., McDonald, D., Knights, D., Reyes, J.A., Clemente, J.C., Burckpile, D.E., Vega Thurber, R.L., Knight, R., Beiko, R.G., 2013. Predictive functional profiling of microbial communities using 16S rRNA marker gene sequences. *Nat. Biotechnol.* 31 (9), 814–821. <https://doi.org/10.1038/nbt.2676>.
- Leininger, S., Ulrich, T., Schlotter, M., Schwark, L., Qi, J., Nicol, G.W., Prosser, J.I., Schuster, S.C., Schleper, C., 2006. Archaea predominate among ammonia-oxidizing prokaryotes in soils. *Nature* 442 (7104), 806–809. <https://doi.org/10.1038/nature04983>.
- Leprich, D.J., Flood, B.E., Schroedl, P.R., Ricci, E., Marlow, J.J., Girguis, P.R., Bailey, J. V., 2021. Sulfur bacteria promote dissolution of authigenic carbonates at marine methane seeps. *ISME J.* 15 (7), 2043–2056. <https://doi.org/10.1038/s41396-021-00903-3>.
- Levićan, G., Ugalde, J.A., Ehrenfeld, N., Maass, A., Parada, P., 2008. Comparative genomic analysis of carbon and nitrogen assimilation mechanisms in three indigenous bioleaching bacteria: predictions and validations. *BMC Genomics* 9 (1), 1–19. <https://doi.org/10.1186/1471-2164-9-581>.
- Liu, Y., Vick-Majors, T.J., Priscu, J.C., Yao, T., Kang, S., Liu, K., Cong, Z., Xiong, J., Li, Y., 2017. Biogeography of cryoconite bacterial communities on glaciers of the Tibetan plateau. *FEMS Microbiol. Ecol.* 93, 6, fix072 <https://doi.org/10.1093/femsec/fix072>.
- Louca, S., Parfrey, L.W., Doebeli, M., 2016. Decoupling function and taxonomy in the global ocean microbiome. *Science* 353 (6305), 1272–1277. <https://doi.org/10.1126/science.aaf4507>.
- Lutz, S., Ziolkowski, L.A., Benning, L.G., 2019. The biodiversity and geochemistry of Cryoconite holes in Queen Maud Land. *East Antarctica. Microorganisms* 7, 160. <https://doi.org/10.3390/microorganisms7060160>.
- MacDonell, S., Sharp, M., Fitzsimons, S., 2016. Cryoconite hole connectivity on the Wright lower glacier, McMurdo dry valleys. *Antarctica. J. Glaciol.* 62 (234), 714–724. <https://doi.org/10.1017/jog.2016.62>.
- Mieczan, T., Górniak, D., Świątecki, A., Zdanowski, M., Tarkowska-Kukuryk, M., 2013. The distribution of ciliates on ecology glacier (King George Island, Antarctica): relationships between species assemblages and environmental parameters. *Polar Biol.* 36, 249–258. <https://doi.org/10.1007/s00300-012-1256-6>.
- Millar, J.L., Bagshaw, E.A., Edwards, A., Poniecka, E.A., Jungblut, A.D., 2021. Polar cryoconite associated microbiota is dominated by hemispheric specialist genera. *Front. Microbiol.* 12 <https://doi.org/10.3389/fmicb.2021.738451>.
- Miot, J., Benzerara, K., Obst, M., Kappler, A., Hegler, F., Schädler, S., Bouche, C., Guyot, F., Morin, G., 2009. Extracellular iron biomineralization by photoautotrophic iron-oxidizing bacteria. *Appl. Environ. Microbiol.* 75 (17), 5586–5591. <https://doi.org/10.1128/AEM.00490-09>.
- Naegeli, K., Huss, M., 2017. Sensitivity of mountain glacier mass balance to changes in bare-ice albedo. *Ann. Glaciol.* 58 (75pt2), 119–129. <https://doi.org/10.1017/aog.2017.25>.
- Nixon, S.L., Telling, J.P., Wadham, J.L., Cockell, C.S., 2017. Viable cold-tolerant iron-reducing microorganisms in geographically diverse subglacial environments. *Biogeosciences* 14(6), 1445–1455. doi:<https://doi.org/10.5194/bg-14-1445-2017>, 2017.
- Nizam, S., Sen, I.S., Vinoj, V., Galy, V., Selby, D., Azam, M.F., Pandey, S.K., Creaser, R.A., Agarwal, A.K., Singh, A.P., Bizimis, M., 2020. Biomass-derived provenance dominates glacial surface organic carbon in the western Himalaya. *Environ. Sci. Technol.* 54 (14), 8612–8621. <https://doi.org/10.1021/acs.est.0c02710>.
- Oerlemans, J., Giesen, R., Van Den Broeke, M., 2009. Retreating alpine glaciers: increased melt rates due to accumulation of dust (Vadret da Morteratsch, Switzerland). *J. Glaciol.* 55 (192), 729–736. <https://doi.org/10.3189/002214309789470969>.
- Olson, M., Rupper, S., 2019. Impacts of topographic shading on direct solar radiation for valley glaciers in complex topography. *Cryosphere* 13, 29–40. <https://doi.org/10.5194/tc-13-29-2019>.
- Oren, A., 2014. The family *Methanoregulaceae*. In: Rosenberg, E., DeLong, E.F., Lory, S., Stackebrandt, E., Thompson, F. (Eds.), *The Prokaryotes*. Springer, Berlin, Heidelberg, pp. 253–258. [https://doi.org/10.1007/978-3-642-38954-2\\_5](https://doi.org/10.1007/978-3-642-38954-2_5).
- Oshkin, I.Y., Beck, D.A., Lamb, A.E., Tchesnokova, V., Benuska, G., McTaggart, T.L., Kalyuzhnaya, M.G., Dedysh, S.N., Lidstrom, M.E., Chistoserdova, L., 2015. Methane fed microcosms show differential community dynamics and pinpoint specific taxa involved in communal response. *ISME J.* 9 (5), 1119–1129. <https://doi.org/10.1038/ismej.2014.203>.
- Pautler, B.G., Dubnick, A., Sharp, M.J., Simpson, A.J., Simpson, M.J., 2013. Comparison of cryoconite organic matter composition from Arctic and Antarctic glaciers at the molecular-level. *Geochim. Cosmochim. Acta* 104, 1–18. <https://doi.org/10.1016/j.gca.2012.11.029>.
- Pester, M., Brambilla, E., Alazard, D., Rattei, T., Weinmaier, T., Han, J., Lucas, S., Lapidus, A., Cheng, J.F., Goodwin, L., Pitluck, S., 2012. Complete genome sequences of *Desulfosporosinus orientis* DSM765T, *Desulfosporosinus youngiae* DSM17734T, *Desulfosporosinus meridiei* DSM13257T, and *Desulfosporosinus acidiphilus* DSM22704T. *J. Bacteriol.* 194, 6300–6301. <https://doi.org/10.1128/JB.01392-12>.

- Pierce, R.W., Turner, J.T., 1992. Ecology of plankton ciliates in marine food webs. *Rev. Aquat. Sci.* 6 (2), 139–181. <https://cir.nii.ac.jp/crid/1572543024330436352>.
- Pittino, F., Zawierucha, K., Poniacka, E., Buda, J., Rosatelli, A., Zordan, S., Azzoni, R.S., Diolaiuti, G., Ambrosini, R., Franzetti, A., 2023. Functional and taxonomic diversity of anaerobes in supraglacial microbial communities. *Microbiol. Spectr.* 11 (2), e0100422 <https://doi.org/10.1128/spectrum.01004-22>.
- Poniacka, E.A., Bagshaw, E.A., Tranter, M., Sass, H., Williamson, C.J., Anesio, A.M., Team, B.A.B., 2018. Rapid development of anoxic niches in supraglacial ecosystems. *Arct. Antarct. Alp. Res.* 50 (1), S100015. <https://doi.org/10.1080/15230430.2017.1420859>.
- Porazinska, D.L., Fountain, A.G., Nysten, T.H., Tranter, M., Virginia, R.A., Wall, D.H., 2004. The biodiversity and biogeochemistry of cryoconite holes from McMurdo Dry Valley glaciers. *Antarctica. Arct. Antarct. Alp. Res.* 36 (1), 84–91. [https://doi.org/10.1657/1523-0430\(2004\)036\[0084:TBABOC\]2.0.CO;2](https://doi.org/10.1657/1523-0430(2004)036[0084:TBABOC]2.0.CO;2).
- Preunkert, S., Legrand, M., Frey, M.M., Kukui, A., Savarino, J., Gallée, H., King, M., Jourdain, B., Vicars, W., Helmig, D., 2015. Formaldehyde (HCHO) in air, snow, and interstitial air at Concordia (East Antarctic plateau) in summer. *Atmos. Chem. Phys.* 15 (12), 6689–6705. <https://doi.org/10.5194/acp-15-6689-2015>.
- Rabus, R., Hansen, T.A., Widdel, F., 2013. Dissimilatory sulfate- and sulfur-reducing prokaryotes. In: Rosenberg, E., DeLong, E.F., Lory, S., Stackebrandt, E., Thompson, F. (Eds.), *The Prokaryotes*. Springer, Berlin, Heidelberg, pp. 309–404. [https://doi.org/10.1007/978-3-642-30141-4\\_70](https://doi.org/10.1007/978-3-642-30141-4_70).
- Rathore, M., Sinha, R.K., Venkatachalam, S., Krishnan, K.P., 2022. Microbial diversity and associated metabolic potential in the supraglacial habitat of a fast-retreating glacier: a case study of Patsio glacier. *Environ. Microbiol. Rep.* North-western Himalaya. <https://doi.org/10.1111/1758-2229.13017>.
- Ren, Z., Gao, H., Luo, W., Elser, J.J., 2022. Bacterial communities in surface and basal ice of a glacier terminus in the headwaters of Yangtze River on the Qinghai-Tibet Plateau. *Environ. microbiome.* 17(1), 1–14. doi:<https://doi.org/10.1186/s40793-022-00408-2>.
- Ricci, C., Balsamo, M., 2000. The biology and ecology of lotic rotifers and gastrotrichs. *Freshw. Biol.* 44 (1), 15–28. <https://doi.org/10.1046/j.1365-2427.2000.00584.x>.
- Rickard, D., 2012. Sulfidic sediments and sedimentary rocks. *Developments in sedimentology*, Vol. 65. Amsterdam: Elsevier.
- Rojas-Jimenez, K., Wurzbacher, C., Bourne, E.C., Chiuchiolo, A., Priscu, J.C., Grossart, H.P., 2017. Early diverging lineages within Cryptomycota and Chytridiomycota dominate the fungal communities in ice-covered lakes of the McMurdo dry valleys, Antarctica. *Sci. Rep.* 10, 7(1), 15348. <https://doi.org/10.1038/s41598-017-15598-w>.
- Rolli, E., Marasco, R., Fusi, M., Scaglia, B., Schubotz, F., Mapelli, F., Ciccazzo, S., Brusetti, L., Trombino, L., Tambone, F., Adani, F., 2022. Environmental micro-niche filtering shapes bacterial pioneer communities during primary colonization of a Himalayas' glacier forefield. *Environ. Microbiol.* 24 (12), 5998–6016. <https://doi.org/10.1111/1462-2920.16268>.
- Samui, G., Antony, R., Mahalinganathan, K., Thamban, M., 2017. Spatial variability and possible sources of acetate and formate in the surface snow of East Antarctica. *J. Environ. Sci.* 57, 258–269. <https://doi.org/10.1016/j.jes.2017.02.003>.
- Samui, G., Antony, R., Thamban, M., 2018. Chemical characteristics of hydrologically distinct cryoconite holes in coastal Antarctica. *Ann. Glaciol.* 59 (77), 69–76. <https://doi.org/10.1017/aog.2018.30>.
- Samui, G., Antony, R., Thamban, M., 2020. Fate of dissolved organic carbon in Antarctic surface environments during summer. *J. Geophys. Res.-Bioge.* 125 (12), e2020JG005958 <https://doi.org/10.1029/2020JG005958>.
- Sanyal, A., Antony, R., Samui, G., Thamban, M., 2018. Microbial communities and their potential for degradation of dissolved organic carbon in cryoconite hole environments of Himalaya and Antarctica. *Microbiol. Res.* 208, 32–42. <https://doi.org/10.1016/j.micres.2018.01.004>.
- Sanyal, A., Antony, R., Ganesan, P., Thamban, M., 2020. Metabolic activity and bioweathering properties of yeasts isolated from different supraglacial environments of Antarctica and Himalaya. *Antonie Van Leeuwenhoek* 113, 2243–2258. <https://doi.org/10.1007/s10482-020-01496-1>.
- Schaner, N., Voisin, N., Nijssen, B., Lettenmaier, D.P., 2012. The contribution of glacier melt to streamflow. *Environ. Res. Lett.* 7 (3), 034029 <https://doi.org/10.1088/1748-9326/7/3/034029>.
- Segawa, T., Ishii, S., Ohte, N., Akiyoshi, A., Yamada, A., Maruyama, F., Li, Z., Hongoh, Y., Takeuchi, N., 2014. The nitrogen cycle in cryoconites: naturally occurring nitrification-denitrification granules on a glacier. *Environ. Microbiol.* 16 (10), 3250–3262. <https://doi.org/10.1111/1462-2920.12543>.
- Segawa, T., Takeuchi, N., Mori, H., Rathnayake, R.M., Li, Z., Akiyoshi, A., Satoh, H., Ishii, S., 2020. Redox stratification within cryoconite granules influences the nitrogen cycle on glaciers. *FEMS. Microb. Ecol.* 96 (11), faa199. <https://doi.org/10.1093/femsec/faa199>.
- Shamurailatpam, M.S., Telling, J., Wadham, J.L., Ramanathan, A., Yates, C.A., Raju, N. J., 2023. Factors controlling the net ecosystem production of cryoconite on Western Himalayan glaciers. *Biogeochemistry* 162, 201–220. <https://doi.org/10.1111/1462-2920.16550>.
- Siegert, M., Atkinson, A., Banwell, A., Brandon, M., Convey, P., Davies, B., Downie, R., Edwards, T., Hubbard, B., Marshall, G., Rogel, J., 2019. The Antarctic peninsula under a 1.5°C global warming scenario. *Front. Environ. Sci.* 7, 102. <https://doi.org/10.3389/fenvs.2019.00102>.
- Simon, C., Wierer, A., Strittmatter, A.W., Daniel, R., 2009. Phylogenetic diversity and metabolic potential revealed in a glacier ice metagenome. *Appl. Environ. Microbiol.* 75 (23), 7519–7526. <https://doi.org/10.1128/AEM.00946-09>.
- Singh, A.T., Laluraj, C.M., Sharma, P., Patel, L.K., Thamban, M., 2017b. Export fluxes of geochemical solutes in the meltwater stream of Sutri Dhaka glacier, Chandra basin, Western Himalaya. *Environ. Monit. Assess.* 189, 1–13. <https://doi.org/10.1007/s10661-017-6268-9>.
- Singh, S.M., Avinash, K., Sharma, P., Mulik, R.U., Upadhyay, A.K., Ravindra, R., 2017a. Elemental variations in glacier cryoconites of Indian Himalaya and Spitsbergen, Arctic. *Geosci. Front.* 8 (6), 1339–1347. <https://doi.org/10.1016/j.gsf.2017.01.002>.
- Smith, D.P., Peay, K.G., 2014. Sequence depth, not PCR replication, improves ecological inference from next generation DNA sequencing. *PLoS One* 9 (2), e90234. <https://doi.org/10.1371/journal.pone.0090234>.
- Sommers, P., Darcy, J.L., Gendron, E.M.S., Stanish, L.F., Bagshaw, E.A., Porazinska, D.L., Schmidt, S.K., 2018. Diversity patterns of microbial eukaryotes mirror those of bacteria in Antarctic cryoconite holes. *FEMS Microbiol. Ecol.* 94,1, fix167 <https://doi.org/10.1093/femsec/fix167>.
- Sommers, P., Porazinska, D.L., Darcy, J.L., Gendron, E.M.S., Vimercati, L., Solon, A.J., Schmidt, S.K., 2020. Microbial Species–Area Relationships in Antarctic Cryoconite Holes Depend on Productivity. *Microorganisms*, 8, 1747. doi:<https://doi.org/10.3390/microorganisms8111747>.
- Sørensen, H.L., Meire, L., Juul-Pedersen, T., de Stigter, H.C., Meysman, F.J., Rysgaard, S., Thamdrup, B., Glud, R.N., 2015. Seasonal carbon cycling in a Greenlandic fjord: an integrated pelagic and benthic study. *Mar. Ecol. Prog. Ser.* 539, 1–17. <https://doi.org/10.3354/meps11503>.
- Stackebrandt, E., Verburg, S., Frühling, A., Busse, H.J., Tindall, B.J., 2009. Dissection of the genus *Methylobium*: reclassification of *Methylobium fulvum* as *Rhizobacter fulvus* comb. nov., *Methylobium aquaticum* as *Piscinibacter aquaticus* gen. nov., comb. nov. and *Methylobium subsaxonicum* as *Rivibacter subsaxonicus* gen. nov., comb. nov. and emended descriptions of the genera *Rhizobacter* and *Methylobium*. *Int. J. Syst. Evol. Microbiol.* 59(10), 2552–2560. doi:<https://doi.org/10.1099/ijs.0.008383-0>.
- Stibal, M., Tranter, M., 2007. Laboratory investigation of inorganic carbon uptake by cryoconite debris from Werenskiöldreen, Svalbard. *Eur. J. Vasc. Endovasc. Surg.* 112 (G4) <https://doi.org/10.1029/2007JG000429>.
- Stibal, M., Tranter, M., Benning, L.G., Reháč, J., 2008. Microbial primary production on an Arctic glacier is insignificant in comparison with allochthonous organic carbon input. *Environ. Microbiol.* 10 (8), 2172–2178. <https://doi.org/10.1111/j.1462-2920.2008a.01620.x>.
- Stieglmeier, M., Klingl, A., Alves, R.J., Rittmann, S.K.M., Melcher, M., Leisch, N., Schleper, C., 2014. *Nitrososphaera viennensis* gen. Nov., sp. nov., an aerobic and mesophilic, ammonia-oxidizing archaeon from soil and a member of the archaeal phylum *Thaumarchaeota*. *Int. J. Syst. Evol. Microbiol.* 64 (Pt 8), 2738–2752. <https://doi.org/10.1099/ijs.0.063172-0>.
- Takeuchi, N., Kohshima, S., Seko, K., 2001. Structure, formation, darkening process of albedo reducing material (cryoconite) on a Himalayan glacier: a granular algal mat growing on the glacier. *Arct. Antarct. Alp. Res.* 33 (2), 115–122. <https://doi.org/10.1080/15230430.2001.12003413>.
- Tapia, J.M., Muñoz, J., González, F., Blázquez, M.L., Ballester, A., 2013. Sorption of ferrous and ferric iron by extracellular polymeric substances (EPS) from acidophilic bacteria. *Prep. Biochem. Biotechnol.* 43 (8), 815–827. <https://doi.org/10.1080/10826068.2013.805624>.
- Telling, J., Anesio, A.M., Hawkings, J., Tranter, M., Wadham, J.L., Hodson, A.J., Irvine-Fynn, T., Yallop, M.L., 2010. Measuring rates of gross photosynthesis and net community production in cryoconite holes: A comparison of field methods. *Ann. Glaciol.* 51 (56), 153–162. <https://doi.org/10.3189/172756411795932056>.
- Telling, J., Anesio, A.M., Tranter, M., Irvine-Fynn, T., Hodson, A., Butler, C., Wadham, J., 2011. Nitrogen fixation on Arctic glaciers, Svalbard. *J. Geophys. Res.* 116 (G3) <https://doi.org/10.1029/2010JG001632>.
- Tieber, A., Lettner, H., Bossew, P., Hubner, A., Sattler, B., Hofmann, W., 2009. Accumulation of anthropogenic radionuclides in cryoconites on alpine glaciers. *J. Environ. Radioact.* 100 (7), 590–598. <https://doi.org/10.1016/j.jenvrad.2009.04.008>.
- Toole, D.R., Zhao, J., Martens-Habbena, W., Strauss, S.L., 2021. Bacterial functional prediction tools detect but underestimate metabolic diversity compared to shotgun metagenomics in Southwest Florida soils. *Appl. Soil Ecol.* 168, 104129 <https://doi.org/10.1016/j.apsoil.2021.104129>.
- Toubes-Rodrigo, M., Potgieter-Vermaak, S., Sen, R., Oddsdóttir, E.S., Elliott, D., Cook, S., 2021. Active microbial ecosystem in glacier basal ice fuelled by iron and silicate comminution-derived hydrogen. *Microbiologyopen* 10 (4), e1200. <https://doi.org/10.1002/mbo3.1200>.
- Tourna, M., Stieglmeier, M., Spang, A., Könneke, M., Schintlmeister, A., Ulrich, T., Engel, M., Schlöter, M., Wagner, M., Richter, A., Schleper, C., 2011. *Nitrososphaera viennensis*, an ammonia oxidizing archaeon from soil. *Proc. Natl. Acad. Sci. USA* 108 (20), 8420–8425. <https://doi.org/10.1073/pnas.1013488108>.
- Vincent, W.F., 2002. Cyanobacterial dominance in the polar regions. In: Whitton, B.A., Potts, M. (Eds.), *The Ecology of Cyanobacteria*. Springer, Dordrecht, pp. 321–340. [https://doi.org/10.1007/0-306-46855-7\\_12](https://doi.org/10.1007/0-306-46855-7_12).
- Vonnahme, T.R., Devetter, M., Žárský, J.D., Šabacká, M., Elster, J., 2016. Controls on microbial community structures in cryoconite holes upon high Arctic glaciers. *Svalbard. Biogeosci. Discuss.* 13 (3), 659–674. <https://doi.org/10.5194/bg-13-659-2016>.
- Ward, T., Larson, J., Meulemans, J., Hillmann, B., Lynch, J., Sidiropoulos, D., Spear, J.R., Caporaso, G., Blekhan, R., Knight, R., Fink, R., 2017. BugBase predicts organism level microbiome phenotypes. *bioRxiv*. [Preprint]. 133462. <https://doi.org/10.1101/133462>.
- Weber, K.A., Achenbach, L.A., Coates, J.D., 2006. Microorganisms pumping iron: anaerobic microbial iron oxidation and reduction. *Nat. Rev. Microbiol.* 4 (10), 752–764. <https://doi.org/10.1038/nrmicro1490>.
- White, T.J., Bruns, T., Lee, S.J.W.T., Taylor, J., 1990. Amplification and direct sequencing of fungal ribosomal RNA genes for phylogenetics. In: Innis, M.A.,

- Gelfand, D.H., Sninsky, J.J., White, T.J. (Eds.), PCR Protocols: A Guide to Methods and Applications. Academic Press, United States, pp. 315–322. <https://doi.org/10.1016/B978-0-12-372180-8.50042-1>.
- Winkel, M., Trivedi, C.B., Mourot, R., Bradley, J.A., Vieth-Hillebrand, A., Benning, L.G., 2022. Seasonality of glacial snow and ice microbial communities. *Front. Microbiol.* 13, 876848 <https://doi.org/10.3389/fmicb.2022.876848>.
- Xu, J., Zhang, Q., Li, X., Ge, X., Xiao, C., Ren, J., Qin, D., 2013. Dissolved organic matter and inorganic ions in a central Himalayan glacier – insights into chemical composition and atmospheric sources. *Environ. Sci. Technol.* 47 (12), 6181–6188. <https://doi.org/10.1021/es4009882>.
- Xu, Y., Simpson, A.J., Eyles, N., Simpson, M.J., 2010. Sources and molecular composition of cryoconite organic matter from the Athabasca glacier. *Canadian Rocky Mountains. Org. Geochem.* 41 (2), 177–186. <https://doi.org/10.1016/j.orggeochem.2009.10.010>.
- Yang, G., Hou, S., Le Baoge, R., Li, Z.G., Xu, H., Liu, Y.P., Du, W.T., Liu, Y.Q., 2016. Differences in bacterial diversity and communities between glacial snow and glacial soil on the Chongce ice cap. *West Kunlun Mountains. Sci. Rep.* 6, 36548. <https://doi.org/10.1038/srep36548>.
- Yu, Z., Chistoserdova, L., 2017. Communal metabolism of methane and the rare earth element switch. *J. Bacteriol.* 199 (22), 10–1128. <https://doi.org/10.1128/JB.00328-17>.
- Zarsky, J.D., Stibal, M., Hodson, A., Sattler, B., Schostag, M., Hansen, L.H., Jacobsen, C. S., Psenner, R., 2013. Large cryoconite aggregates on a Svalbard glacier support a diverse microbial community including ammonia-oxidizing archaea. *Environ. Res. Lett.* 8, 035044 <https://doi.org/10.1088/1748-9326/8/3/035044>.
- Zawierucha, K., Ostrowska, M., Vonnahme, T.R., Devetter, M., Nawrot, A., Lehmann, S., Koliczka, M., 2016. Diversity and distribution of Tardigrada in Arctic cryoconite holes. *J. Limnol.* 75 (3), 545–559. <https://doi.org/10.4081/jlimnol.2016.1453>.
- Zawierucha, K., Porazinska, D.L., Ficaretola, G.F., Ambrosini, R., Baccolo, G., Buda, J., Ceballos, J.L., Devetter, M., Dial, R., Franzetti, A., Fuglewicz, U., Gielly, L., Łokas, E., Janko, K., Novotna Jaromerska, T., Kościński, A., Kozłowska, A., Ono, M., Parnikoza, I., Pittino, F., Poniecka, E., Sommers, P., Schmidt, S.K., Shain, D., Sikorska, S., Uetake, J., Takeuchi, N., 2021. A hole in the nematosphere: tardigrades and rotifers dominate the cryoconite hole environment, whereas nematodes are missing. *J. Zool.* 313, 18–36. <https://doi.org/10.1111/jzo.12832>.
- Zdanowski, M.K., Bogdanowicz, A., Gawor, J., Gromadka, R., Wolicka, D., Grzesiak, J., 2017. Enrichment of Cryoconite hole anaerobes: implications for the subglacial microbiome. *Microb. Ecol.* 73, 532–538. <https://doi.org/10.1007/s00248-016-0886-6>.
- Zeng, J., Lou, K., Zhang, C.J., Wang, J.T., Hu, H.W., Shen, J.P., Zhang, L.M., Han, L.L., Zhang, T., Lin, Q., Chalk, P.M., 2016. Primary succession of nitrogen cycling microbial communities along the Deglaciated forelands of Tianshan Mountain. *China. Front. Microbiol.* 7, 1353. <https://doi.org/10.3389/fmicb.2016.01353>.
- Zhang, L., Delgado-Baquerizo, M., Hotaling, S., Li, Y., Sun, X., Xu, Y., Chu, H., 2023. Bacterial diversity and co-occurrence patterns differ across a world-wide spatial distribution of habitats in glacier ecosystems. *Funct. Ecol.* 37 (6), 1520–1535. <https://doi.org/10.1111/1365-2435.14317>.